



Measurement of jet fragmentation in 5.02 TeV proton–lead and proton–proton collisions with the ATLAS detector

The ATLAS Collaboration *

Received 11 July 2018; received in revised form 11 July 2018; accepted 11 July 2018

Available online 17 July 2018

Abstract

A measurement of the fragmentation functions of jets into charged particles in $p + \text{Pb}$ collisions and pp collisions is presented. The analysis utilizes 28 nb^{-1} of $p + \text{Pb}$ data and 26 pb^{-1} of pp data, both at $\sqrt{s_{\text{NN}}} = 5.02 \text{ TeV}$, collected in 2013 and 2015, respectively, with the ATLAS detector at the LHC. The measurement is reported in the centre-of-mass frame of the nucleon–nucleon system for jets in the rapidity range $|y^*| < 1.6$ and with transverse momentum $45 < p_{\text{T}} < 260 \text{ GeV}$. Results are presented both as a function of the charged-particle transverse momentum and as a function of the longitudinal momentum fraction of the particle with respect to the jet. The pp fragmentation functions are compared with results from Monte Carlo event generators and two theoretical models. The ratios of the $p + \text{Pb}$ to pp fragmentation functions are found to be consistent with unity.

© 2018 CERN for the benefit of the ATLAS Collaboration. Published by Elsevier B.V. This is an open access article under the CC BY license (<http://creativecommons.org/licenses/by/4.0/>).

Keywords: Relativistic heavy-ion collisions; Jets; Fragmentation into hadrons

1. Introduction

Heavy-ion collisions at the Large Hadron Collider (LHC) are performed in order to produce and study the quark–gluon plasma (QGP), a phase of strongly interacting matter which emerges at very high energy densities; a recent review can be found in Ref. [1]. Measurements of jets and jet properties in heavy-ion collisions are sensitive to the properties of the QGP. In order to quantify jet modifications in heavy-ion collisions, proton–proton (pp) collisions are often used as a

* E-mail address: atlas.publications@cern.ch.

reference system. Using this reference, rates of jet production in Pb + Pb collisions are observed to be reduced compared to that expected from the rates in pp collisions, appropriately scaled to account for the nuclear thickness in Pb + Pb collisions [2,3]. Charged-particle fragmentation functions are also observed to be modified in Pb + Pb collisions compared to pp collisions [4–6]. Both of these effects are interpreted as arising predominantly from the modification of the parton showering process in the final stages of the collision.

In addition to final-state differences emerging from the presence of the hot and dense matter, jet production in Pb + Pb collisions may also differ from that in pp collisions due to effects arising from the presence of the large nucleus. For example, nucleons bound in a nucleus are expected to have a modified structure compared to the free nucleon [7], and partons may lose energy in the nuclear environment before scattering [8]. Proton–nucleus collisions are used to differentiate between initial- and final-state effects in Pb + Pb collisions. The inclusive jet production rate in proton–lead ($p + \text{Pb}$) collisions at 5.02 TeV was measured [9–11] at the LHC and found to be only slightly modified after normalization by the nuclear thickness function. Measurements made at the Relativistic Heavy Ion Collider with deuteron–gold collisions yield similar results [12] (interestingly, Refs. [9,12] observe a centrality dependence to inclusive jet production). High transverse momentum (p_T) charged hadrons originate from the fragmentation of jets and provide a complementary observable to that of jet production. The CMS Collaboration observed a small excess in the charged-particle spectrum measured in $p + \text{Pb}$ collisions for $p_T > 20$ GeV particles compared to that expected from pp collisions [13]. Measurements of charged-particle fragmentation functions for jets in different p_T intervals in $p + \text{Pb}$ and pp collisions are crucial for connecting the jet and charged-particle results. Therefore, the measurements reported here are necessary both to establish a reference for jet fragmentation measurements in Pb + Pb collisions and to determine any modifications to jet fragmentation in $p + \text{Pb}$ collisions due to the presence of a large nucleus.

In recent years many of the features of Pb + Pb collisions which were interpreted as final state effects due to hot nuclear matter were also observed in $p + \text{Pb}$ collisions at the LHC and in $d + \text{Au}$ collisions at RHIC. These features include long-range hadron correlations [14–17] and a centrality-dependent reduction in the quarkonia yields [18–21]. There is considerable debate about whether these features arise from the same source as in Pb + Pb collisions [22] or from other effects such as initial state gluon saturation [23]. Measurements of jets in $p + \text{Pb}$ collisions showed no effects that would be attributable to hot nuclear matter, however additional measurements of jet properties in these collisions could help to constrain the source of the modifications observed in other observables.

In this paper, the jet momentum structure in pp and $p + \text{Pb}$ collisions is studied using the distributions of charged particles associated with jets which have a transverse momentum p_T^{jet} in the range 45 to 260 GeV. Jets are reconstructed with the anti- k_t algorithm [24] using a radius parameter $R = 0.4$. Charged particles are assigned to jets via an angular matching $\Delta R < 0.4$,¹ where ΔR is the angular distance between the jet axis and the charged-particle position. Results on the fragmentation functions are presented both as a function of the ratio between the

¹ ATLAS uses a right-handed coordinate system with its origin at the nominal interaction point (IP) in the centre of the detector and the z -axis along the beam pipe. The x -axis points from the IP to the centre of the LHC ring, and the y -axis points upward. Cylindrical coordinates (r, ϕ) are used in the transverse plane, ϕ being the azimuthal angle around the beam pipe. The pseudorapidity is defined in terms of the polar angle θ as $\eta = -\ln \tan(\theta/2)$. Rapidity is defined as $y = 0.5 \ln \frac{E+p_z}{E-p_z}$ where E and p_z are the energy and the component of the momentum along the beam direction. Angular distance is measured in units of $\Delta R \equiv \sqrt{(\Delta\eta)^2 + (\Delta\phi)^2}$.

component of the particle transverse momentum parallel to the jet direction, and the jet p_T , $z \equiv p_T \cos \Delta R / p_T^{\text{jet}}$,² and as a function of the charged-particle transverse momentum with respect to the beam direction, p_T :

$$D(z) \equiv \frac{1}{N_{\text{jet}}} \frac{dN_{\text{ch}}}{dz}, \quad (1)$$

and

$$D(p_T) \equiv \frac{1}{N_{\text{jet}}} \frac{dN_{\text{ch}}}{dp_T}. \quad (2)$$

The quantity N_{ch} is the number of charged particles and N_{jet} is the number of jets under consideration. The fragmentation functions are per-jet normalized.

The fragmentation functions are compared in $p + \text{Pb}$ and pp collisions at a centre-of-mass energy of 5.02 TeV. In order to quantify any difference between $p + \text{Pb}$ and pp collisions, the ratios of the fragmentation functions are measured:

$$R_{D(z)} \equiv \frac{D(z)_{p\text{Pb}}}{D(z)_{pp}}. \quad (3)$$

In $\text{Pb} + \text{Pb}$ collisions, such measurements are also presented as a function of charged-particle p_T [4,6] to explore the absolute p_T scale of the modifications and to reduce jet-related uncertainties. Thus, in addition to the more commonly used fragmentation functions as a function of z , this paper also presents the analogous distributions and their ratios as a function of charged particle p_T :

$$R_{D(p_T)} \equiv \frac{D(p_T)_{p\text{Pb}}}{D(p_T)_{pp}}. \quad (4)$$

2. Experimental set-up

The measurements presented here are performed using the ATLAS calorimeter, inner detector, trigger, and data acquisition systems [25]. The calorimeter system consists of a sampling liquid argon (LAr) electromagnetic (EM) calorimeter covering $|\eta| < 3.2$, a steel–scintillator sampling hadronic calorimeter covering $|\eta| < 1.7$, a LAr hadronic calorimeter covering $1.5 < |\eta| < 3.2$, and two LAr forward calorimeters (FCal) covering $3.2 < |\eta| < 4.9$. The hadronic calorimeter has three sampling layers longitudinal in shower depth. The EM calorimeters are segmented longitudinally in shower depth into three layers plus an additional pre-sampler layer. The EM calorimeter has a granularity that varies with layer and pseudorapidity, but which is generally much finer than that of the hadronic calorimeter. The minimum-bias trigger scintillators (MBTS) [25] detect charged particles over $2.1 < |\eta| < 3.9$ using two segmented counters placed at $z = \pm 3.6$ m. Each counter provides measurements of both the pulse heights and the arrival times of ionization energy deposits.

A two-level trigger system was used to select the $p + \text{Pb}$ and pp collisions analysed here. The first, the hardware-based trigger stage Level-1, is implemented with custom electronics. The second level is the software-based High Level Trigger (HLT). Jet events were selected by the HLT with Level-1 seeds from jet, minimum-bias, and total-energy triggers. The total-energy trigger

² The ΔR is an approximation of the opening angle $\sqrt{(\Delta\theta)^2 + (\Delta\phi)^2}$.

required a total transverse energy measured in the calorimeter of greater than 5 GeV. The HLT jet trigger operated a jet reconstruction algorithm similar to that applied in the offline analysis and selected events containing jets with transverse energy thresholds ranging from 20 GeV to 75 GeV in $p + \text{Pb}$ collisions and up to 85 GeV in pp collisions. In both the pp and $p + \text{Pb}$ collisions, the highest-threshold jet trigger sampled the full delivered luminosity. Minimum-bias $p + \text{Pb}$ events were required to have at least one hit in a counter on each side of the MBTS detector at the Level-1 trigger.

The inner detector measures charged-particle tracks within the pseudorapidity interval $|\eta| < 2.5$ using a combination of silicon pixel detectors, silicon microstrip detectors (SCT), and a straw-tube transition radiation tracker (TRT), all immersed in a 2 T axial magnetic field [25]. Each of the three detectors is composed of a barrel and two symmetric end-cap sections. The pixel detector is composed of three layers of sensors with a nominal pixel size of $50 \mu\text{m} \times 400 \mu\text{m}$. Following the $p + \text{Pb}$ data-taking and prior to the 5 TeV pp data-taking an additional silicon tracking layer, the “insertable B-layer” (IBL) [26], was installed closer to the interaction point than the other three layers. The SCT barrel section contains four layers of modules with $80 \mu\text{m}$ pitch sensors on both sides, and each end-cap consists of nine layers of double-sided modules with radial strips having a mean pitch of $80 \mu\text{m}$. The two sides of each SCT layer in both the barrel and the end-caps have a relative stereo angle of 40 mrad. The TRT contains up to 73 (160) layers of staggered straws interleaved with fibres in the barrel (end-cap).

3. Event selection and data sets

The $p + \text{Pb}$ data used in this analysis were recorded in 2013. The LHC was configured with a 4 TeV proton beam and a 1.57 TeV per nucleon Pb beam producing collisions with $\sqrt{s_{\text{NN}}} = 5.02$ TeV and a rapidity shift of the centre-of-mass frame, $\Delta y = 0.465$, relative to the laboratory frame. The data collection was split into two periods with opposite beam configurations. The first period consists of approximately 55% of the integrated luminosity with the Pb beam travelling toward positive rapidity and the proton beam to negative rapidity. The remaining data were taken with the beams of protons and Pb nuclei swapped. The total $p + \text{Pb}$ integrated luminosity is 28 nb^{-1} . Approximately 26 pb^{-1} of $\sqrt{s} = 5.02$ TeV pp data from 2015 was used. The instantaneous luminosity conditions provided by the LHC resulted in an average number of $p + \text{Pb}$ interactions per bunch crossing of 0.03. During pp data-taking, the average number of interactions per bunch crossing varied from 0.6 to 1.3.

The $p + \text{Pb}$ events selected are required to have a reconstructed vertex, at least one hit in each MBTS detector, and a time difference measured between the two MBTS sides of less than 10 ns. The pp events used in this analysis are required to have a reconstructed vertex; no requirement on the signal in the MBTS detector is imposed. In $p + \text{Pb}$ collisions the event centrality is determined by the FCal in the Pb-going direction as in Ref. [9]. The $p + \text{Pb}$ events used here belong to the 0–90% centrality interval.

The performance of the ATLAS detector and offline analysis in measuring fragmentation functions in $p + \text{Pb}$ collisions is evaluated using a sample of Monte Carlo (MC) events obtained by overlaying simulated hard-scattering pp events generated with PYTHIA version 6.423 (PYTHIA6) [27] onto minimum-bias $p + \text{Pb}$ events recorded during the same data-taking period. A sample consisting of 2.4×10^7 pp events is generated with PYTHIA6 using parameter values from the AUET2B tune [28] and the CTEQ6L1 parton distribution function (PDF) set [29], at $\sqrt{s} = 5.02$ TeV and with a rapidity shift equivalent to that in the $p + \text{Pb}$ collisions is used in the overlay procedure. About half of the events are simulated with one beam configuration

and the second half with the other. The detector response is simulated using GEANT4 [30,31], and the simulated hits are combined with those from the data event. An additional sample of 2.6×10^7 pp hard-scattering events simulated with PYTHIA version 8.212 (PYTHIA8) [32] at $\sqrt{s} = 5.02$ TeV with the A14 tune [33] and NNPDF23LO PDF set [34] is used to evaluate the performance for measuring fragmentation functions in the 2015 pp data. Finally, fragmentation functions at generator-level evaluated from 1.5×10^7 5.02 TeV pp events [35] generated with HERWIG++ using the UEEE5 tune [36] and the CTEQ6L1 PDFs [29] are compared to the fragmentation function measured in 5.02 TeV pp data.

4. Jet and track selection

Jets are reconstructed with the same heavy-ion jet reconstruction algorithm used in previous measurements in $p + \text{Pb}$ collisions [9]. The anti- k_T algorithm [24] is first run in four-momentum recombination mode using as input the signal in $\Delta\eta \times \Delta\phi = 0.1 \times 0.1$ calorimeter towers with the anti- k_T radius parameter R set to 0.4 and 0.2 ($R = 0.4$ jets are used for the main analysis and the $R = 0.2$ jets are used to improve the jet position resolution as discussed below). The energies in the towers are obtained by summing the energies of calorimeter cells at the electromagnetic energy scale within the tower boundaries. Then, an iterative procedure is used to estimate the layer- and η -dependent underlying event (UE) transverse energy density, while excluding the regions populated by jets. The UE transverse energy is subtracted from each calorimeter cell and the four-momentum of the jet is updated accordingly. Then, a jet η - and p_T -dependent correction factor derived from the simulation samples is applied to correct the jet momentum for the calorimeter response. Additionally, the jet energies were corrected by a multiplicative factor derived in *in situ* studies of the transverse momentum balance of jets recoiling against photons, Z bosons, and jets in other regions of the calorimeter [37,38]. This *in situ* calibration, which typically differed from unity by a few percent, accounts for differences between the simulated detector response and data.

Jets are required to have jet centre-of-mass rapidity, $|y_{\text{jet}}^*| < 1.6$,³ which is the largest symmetric overlap between the two collision systems for which there is full charged-particle tracking coverage within a jet cone of size $R = 0.4$. To prevent neighbouring jets from distorting the measurement of the fragmentation functions, jets are rejected if there is another jet with higher p_T within a distance $\delta R = 1.0$, where δR is the distance between the two jet axes. To reduce the effects of the broadening of the jet position measurement due to the UE, for $R = 0.4$ jets, the jet direction is taken from that of the closest matching $R = 0.2$ jet within $\delta R = 0.3$ when such a matching jet is found (this procedure has been previously used in Ref. [5]). All jets included in the analysis are required to have p_T sufficiently large for the jet trigger efficiency to be higher than 99%. Reconstructed jets which consist only of isolated high- p_T electrons [39] from electroweak bosons are excluded from this analysis.

The MC samples are used to evaluate the jet reconstruction performance and to correct the measured distributions for detector effects. The $p + \text{Pb}$ jet reconstruction performance is described in Ref. [9]; the jet reconstruction performance in pp collisions is found to be similar to that in $p + \text{Pb}$ collisions. In the MC samples, the kinematics of the particle-level jets are re-

³ The jet centre-of-mass rapidity y_{jet}^* is defined as $y_{\text{jet}}^* \equiv y_{\text{jet}} - \Delta y$ where y_{jet} is the jet rapidity in the ATLAS rest frame and Δy is the rapidity shift of the centre-of-mass frame.

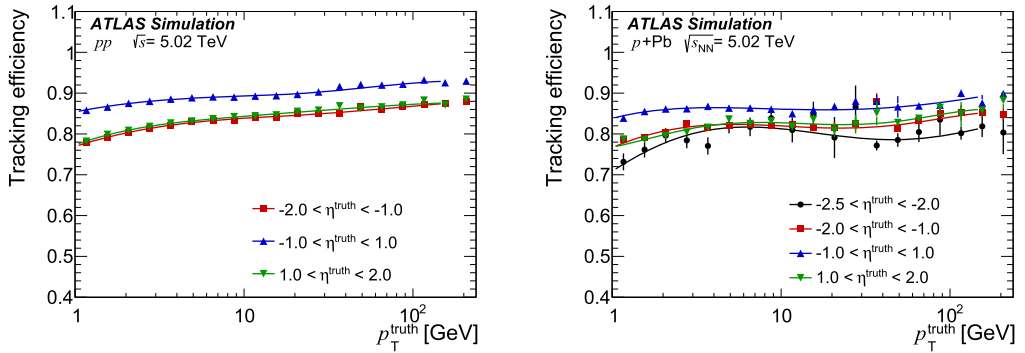


Fig. 1. Tracking efficiency as a function the primary particle momentum at generation level, p_T^{truth} , in pp collisions (left) and in $p + \text{Pb}$ collisions for one of the two beam configurations (right). The different sets of points show the primary particle pseudorapidity, η^{truth} , intervals in which the track reconstruction efficiency has been performed. The different η^{truth} intervals in pp and $p + \text{Pb}$ plots reflect the different regions of the tracking system used in the two cases due to the boosted $p + \text{Pb}$ system. The solid curves show parameterizations of efficiencies.

constructed from primary particles⁴ with the anti- k_t algorithm with radius parameter $R = 0.4$. In these studies, particle-level jets are matched to reconstructed jets with a $\Delta R < 0.2$.

Tracks used in the analysis of $p + \text{Pb}$ collisions are required to have at least one hit in the pixel detector and at least six hits in the SCT. Tracks used in the analysis of pp collisions are required to have at least 9 or 11 total silicon hits for $|\eta| < 1.65$ or $|\eta| > 1.65$, respectively, including both the pixel layers and the SCT. This includes a hit in the first (first or second) pixel layer if expected from the track trajectory for the $p + \text{Pb}$ (pp) data. All tracks used in this analysis are required to have $p_T > 1$ GeV. In order to suppress the contribution of secondary particles, the distance of closest approach of the track to the primary vertex is required to be less than 1.5 mm along the beam axis and less than a value which varies from approximately 0.6 mm at $p_T = 1$ GeV to approximately 0.2 mm at $p_T = 20$ GeV in the transverse plane.

The efficiency for reconstructing charged particles within jets in $p + \text{Pb}$ and pp collisions is evaluated using PYTHIA6 and PYTHIA8 MC samples, respectively, and is computed by matching the reconstructed tracks to generator-level primary particles. The association is done based on contributions of generator-level particles to the hits in the detector layers. A reconstructed track is matched to a generator-level particle if it contains hits produced primarily by this particle [31]. The efficiencies are determined separately for the two $p + \text{Pb}$ running configurations because the η regions of the detector used for the track measurement are different for the two beam configurations. The charged-particle reconstruction efficiencies as a function of the primary particle's transverse momentum, p_T^{truth} , in coarse η^{truth} intervals, are shown in Fig. 1 in pp and $p + \text{Pb}$ collisions. The p_T^{truth} dependence of the efficiencies is parameterized using a fifth-order polynomial in $\log(p_T^{\text{truth}})$ which describes the efficiency behaviour in the range of particle p_T^{truth} from 1.0 to 150 GeV. The tracking efficiency is observed to be constant above 150 GeV and a constant efficiency value is used for particles with $p_T^{\text{truth}} > 150$ GeV due to the limited size of the MC samples in that phase space region. To account for finer scale variations of the tracking efficiency with pseudorapidity, the parameterizations are multiplied by an η -dependent scale factor

⁴ Primary particles are defined as particles with a mean lifetime $\tau > 0.3 \times 10^{-10}$ s either directly produced in pp interactions or from subsequent decays of particles with a shorter lifetime. All other particles are considered to be secondary.

evaluated in η^{truth} intervals of 0.1 units in coarse $p_{\text{T}}^{\text{truth}}$ intervals. The dependence of the charged-particle efficiency on $p_{\text{T}}^{\text{jet}}$ is found to be negligible for the $p_{\text{T}}^{\text{jet}}$ selections used here. The measured $D(z)$ and $D(p_{\text{T}})$ distributions are corrected for the contribution of reconstructed “fake” tracks which cannot be matched to a generated primary particle in the MC samples produced without minimum bias interactions overlaid and the residual contribution of tracks matched to secondary particles. The fraction of secondary and fake tracks is found to be below 2% of the tracks that pass the selection in any track and jet kinematic region. The contribution from these tracks to the fragmentation functions is subtracted from the measured fragmentation functions in both the $p\text{p}$ and $p + \text{Pb}$ collisions.

5. Analysis procedure

Reconstructed charged particle tracks are associated with a reconstructed jet if they fall within $\Delta R = 0.4$ of the jet axis. For each of these particles the momentum fraction, z , is calculated. The measured fragmentation functions are constructed as:

$$D(z)_{\text{meas}} \equiv \frac{1}{N_{\text{jet}}} \frac{1}{\varepsilon(\eta, p_{\text{T}})} \frac{\Delta N_{\text{ch}}(z)}{\Delta z} \quad (5)$$

and

$$D(p_{\text{T}})_{\text{meas}} \equiv \frac{1}{N_{\text{jet}}} \frac{1}{\varepsilon(\eta, p_{\text{T}})} \frac{\Delta N_{\text{ch}}(p_{\text{T}})}{\Delta p_{\text{T}}}, \quad (6)$$

where $\varepsilon(\eta, p_{\text{T}})$ is the track reconstruction efficiency, and N_{jet} is the total number of jets in a given $p_{\text{T}}^{\text{jet}}$ bin. The quantities $\Delta N_{\text{ch}}(z)$ and $\Delta N_{\text{ch}}(p_{\text{T}})$ are the numbers of associated tracks within the given z or p_{T} range, respectively. The efficiency correction is applied on a track-by-track basis, assuming $p_{\text{T}} = p_{\text{T}}^{\text{truth}}$. While that assumption is not strictly valid, the efficiency varies sufficiently slowly with $p_{\text{T}}^{\text{truth}}$ that the error introduced by this assumption is negligible.

In $p + \text{Pb}$ collisions the UE contribution to the fragmentation functions from charged particles not associated with the jet constitutes a background that needs to be subtracted. It originates in soft interactions that accompany the hard process in the same $p + \text{Pb}$ collision and depends on charged-particle p_{T} and η . This background is determined event by event for each measured jet by using a grid of $\Delta R = 0.4$ cones that span the full coverage of the inner detector. The cones have a fixed distance between their centres chosen such that the coverage of the inner detector is maximized while the cones do not overlap each other. Any such cone containing a charged particle with $p_{\text{T}} > 3.5$ GeV is assumed to be associated with a real jet and is excluded from the UE contribution. The 3.5 GeV threshold is derived from studies of UE contribution in MC samples. The estimated contribution from UE particles in each cone is corrected to account for differences in the average UE particle yield at a given p_{T} between the η position of the cone and the η position of the jet. The correction is based on a parameterization of the p_{T} and η dependence of charged-particle yields in minimum-bias collisions. The resulting UE contribution is evaluated for charged particles in the transverse momentum interval of $1 < p_{\text{T}} < 3.5$ GeV and averaged over all cones. The UE contribution is further corrected for the correlation between the actual UE yield within the jet cone and the jet energy resolution discussed in Ref. [5]. This effect is corrected by a multiplicative correction factor, dependent on the track p_{T} (or z) and the jet p_{T} . The correction is estimated in MC samples as the ratio of the UE contribution calculated from tracks within the area of a jet that do not have an associated generator-level particle to the UE contribution estimated by the cone method. Corrected UE contributions are then subtracted from

measured distributions. The maximum size of the UE contribution is 20% for the lowest track p_T (or z). The UE from the cone method is compared to an alternative UE estimation and the difference is found to be negligible. The subtracted UE contribution has no azimuthal variation in $p + \text{Pb}$ collisions and no UE subtraction is performed for the pp measurement due to negligible UE contribution (less than 2% over the entire kinematic range measured).

The measured $D(z)$ and $D(p_T)$ distributions are corrected for detector effects by means of a two-dimensional Bayesian unfolding procedure [40] using the RooUnfold package [41]. The unfolding procedure removes the effect of bin migration due to the jet energy and the track momentum resolutions. Using the MC samples, four-dimensional response matrices are created using the particle-level and reconstructed p_T^{jet} , and generator-level and reconstructed track $p_T(z)$. Separate unfolding matrices are constructed for the $p + \text{Pb}$ and pp data. An independent bin-by-bin unfolding procedure is used to correct the measured p_T^{jet} spectra, which is used to normalize the unfolded fragmentation functions by the number of jets. The response matrices are reweighted such that the shapes of the measured fragmentation functions and jet spectra in the simulation match those in the data. The number of iterations in the Bayesian unfolding is selected to be the minimum number for which the relative change in the fragmentation function at $z = 0.1$ is smaller than 0.2% per additional iteration in all p_T^{jet} bins. This condition ensures the stability of the unfolding and minimizes statistical fluctuations due to the unfolding in the high z and p_T regions. The resulting number of iterations is driven by the low p_T^{jet} intervals, which require the most iterations to converge. The systematic uncertainty due to the unfolding is typically much larger than the impact of the stability requirement, especially for the lowest p_T^{jet} values used in this analysis (discussed in Section 6). Following this criterion, 14 iterations are used for both the $p + \text{Pb}$ and pp data sets. The analysis procedure is tested by dividing the MC event sample in half and using one half to generate response matrices with which the other half is unfolded. Good recovery of the generator-level distributions is observed for the unfolded events and the deviations from perfect closure are incorporated into the systematic uncertainties.

6. Systematic uncertainties

The systematic uncertainties in the measurement of the fragmentation functions and their ratios are described in this section. The following sources of systematic uncertainty in the measurement of the fragmentation functions and their ratios are considered: the jet energy scale (JES), the jet energy resolution (JER), the dependence of the unfolded results on the choice of the starting MC distributions, the residual non-closure of the unfolding and the tracking-related uncertainties. For each variation reflecting a systematic uncertainty the fragmentation functions are re-evaluated and the difference between the varied and nominal fragmentation functions is used as an estimate of the uncertainty. The systematic uncertainties in the $D(z)$ and $D(p_T)$ measurements in both collision systems are summarized in Figs. 2 and 3, respectively, for two different jet p_T bins. The systematic uncertainties from each source are taken as uncorrelated and combined in quadrature to obtain the total systematic uncertainty.

The JES uncertainty is determined from *in situ* studies of the calorimeter response [37,42, 43], and studies of the relative energy-scale difference between the jet reconstruction procedure in heavy-ion collisions and the procedure used in pp collisions [44]. The impact of the JES uncertainty on the measured distributions is evaluated by constructing new response matrices where all reconstructed jet transverse momenta are shifted by ± 1 standard deviation ($\pm 1\sigma$) of the JES uncertainty. The data are then unfolded with these matrices. Each component that contributes

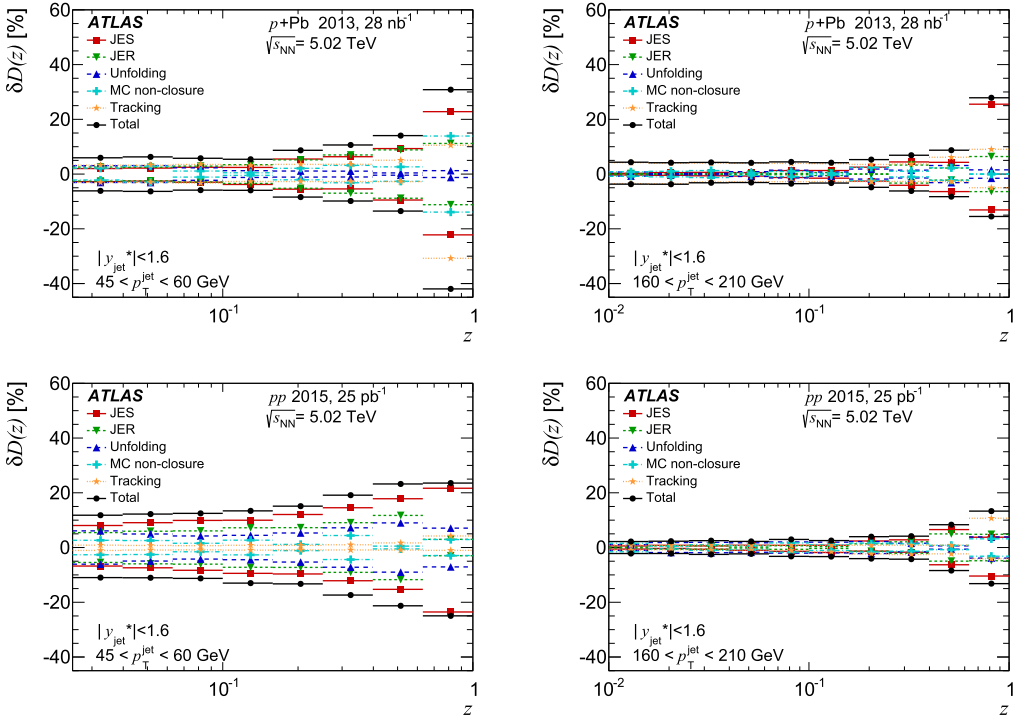


Fig. 2. Summary of the systematic uncertainties in the fragmentation function, $D(z)$, in $p + \text{Pb}$ collisions (top) and pp collisions (bottom) for jets in the 45–60 GeV $p_{\text{T}}^{\text{jet}}$ interval (left) and in the 160–210 GeV $p_{\text{T}}^{\text{jet}}$ interval (right). The systematic uncertainties due to JES, JER, unfolding, MC non-closure and tracking are shown along with the total systematic uncertainty from all sources.

to the JES uncertainty is varied separately. In total, 45 and 51 independent systematic components constitute the full JES uncertainty in the analysis of $p + \text{Pb}$ and pp collisions, respectively. These components are uncorrelated among each other within the data set and fully correlated across p_{T} and η . The JES uncertainty increases with increasing z and particle p_{T} at fixed $p_{\text{T}}^{\text{jet}}$ and decreases with increasing $p_{\text{T}}^{\text{jet}}$.

The uncertainty in the fragmentation functions due to the JER is estimated by repeating the unfolding procedure with modified response matrices, where the resolution of the reconstructed jet $p_{\text{T}}^{\text{jet}}$ is broadened by Gaussian smearing. The smearing factor is evaluated using an *in situ* technique involving studies of dijet energy balance [45,46]. The systematic uncertainty due to the JER increases with increasing z and particle p_{T} at fixed $p_{\text{T}}^{\text{jet}}$ and decreases with increasing $p_{\text{T}}^{\text{jet}}$.

The unfolding uncertainty is estimated by generating the response matrices from the MC distributions without reweighting to match the shapes of the reconstructed data in $p_{\text{T}}^{\text{jet}}$ and $D(z)$ or $D(p_{\text{T}})$. Conservatively, an additional uncertainty to account for possible residual limitations in the analysis procedure was assigned by evaluating the non-closure of the unfolded distributions in simulations, as described in Section 5. The magnitude of both of these uncertainties is typically below 5% except for the highest z and track p_{T} bins.

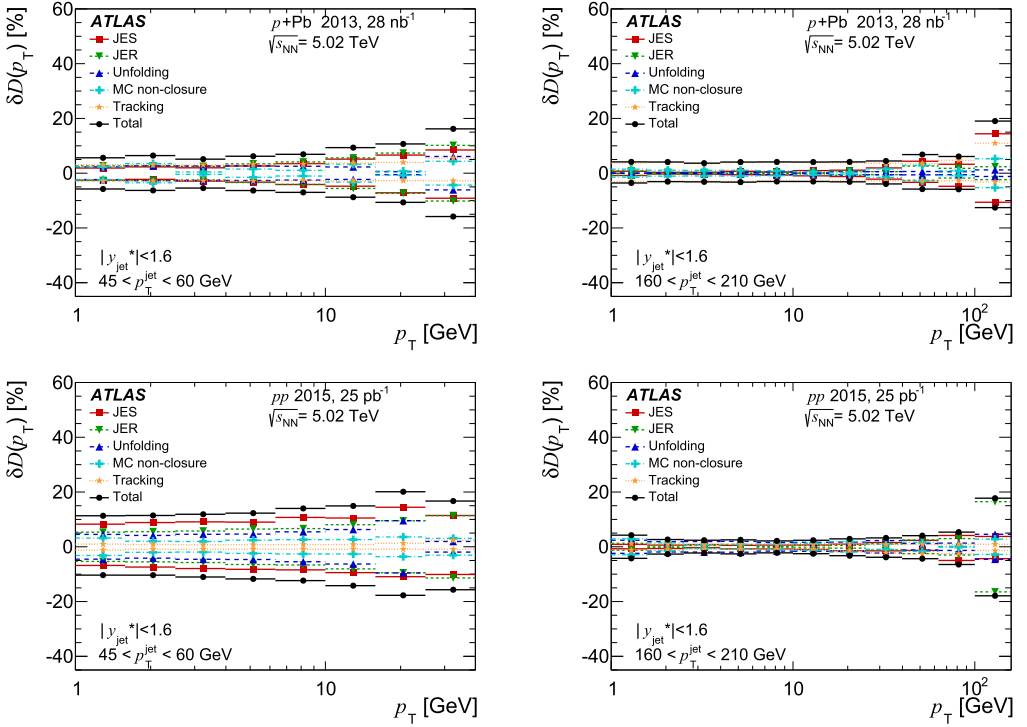


Fig. 3. Summary of the systematic uncertainties in the fragmentation function, $D(p_T)$, in $p + \text{Pb}$ collisions (top) and pp collisions (bottom) for jets in the 45–60 GeV p_T^{jet} interval (left) and in the 160–210 GeV p_T^{jet} interval (right). The systematic uncertainties due to JES, JER, unfolding, MC non-closure and tracking are shown along with the total systematic uncertainty from all sources.

The uncertainties related to the track reconstruction and selection originate from several sources. Uncertainties related to the rate of secondary and fake tracks, the material description in the simulation, and the track's transverse momentum were obtained from studies in data and simulation described in Ref. [47]. The systematic uncertainty in the secondary-track and fake-track rate is 30% in pp collisions and 50% in $p + \text{Pb}$. The contamination by secondary and fake tracks is at most 2%, the resulting uncertainty in the fragmentation functions is at most 1%. The sensitivity of the tracking efficiency to the description of the inactive material in the MC samples is evaluated by varying the material description. This uncertainty is between 0.5 and 2% (depending on track η) in the track p_T range used in the analysis. Uncertainty in the tracking efficiency due to the high local track density in the cores of jets is 0.4% [48] for all p_T^{jet} selections in this analysis. The uncertainty due to the track selection criteria is evaluated by repeating the analysis with an additional requirement on the significance of the distance of closest approach of the track to the primary vertex. This uncertainty affects both the track reconstruction efficiency and the rate of secondary and fake tracks. The resulting uncertainty typically varies from 1% at low track p_T and low z to 5% at high track p_T and high z . The systematic uncertainties in the fragmentation functions due to the parameterization of the efficiency corrections is less than 1%. An additional uncertainty takes into account a possible residual misalignment of the tracking detectors in pp data-taking. The alignment in this data was checked *in situ* with $Z \rightarrow \mu^+ \mu^-$

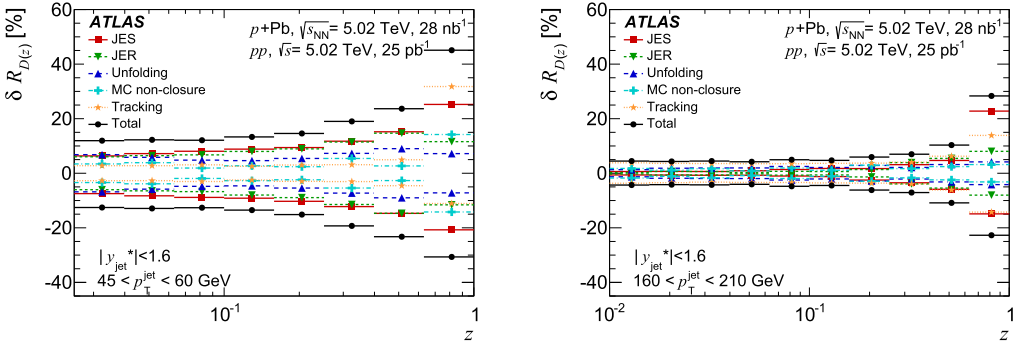


Fig. 4. Summary of the systematic uncertainties for $R_{D(z)}$ ratios, for jets in the 45–60 GeV p_T interval (left) and in the 160–210 GeV p_T interval (right). The systematic uncertainties due to JES, JER, unfolding, MC non-closure and tracking are shown along with the total systematic uncertainty from all sources.

events, and thus a track- p_T -dependent uncertainty arises from the finite size of this sample. The resulting uncertainties in the fragmentation functions are typically smaller than 1% except at large z where they are as large as 4%. Finally, the track-to-particle matching requirements are varied. This variation affects the track reconstruction efficiency, the track momentum resolution, and the rate of secondary and fake tracks. The resulting uncertainties in the fragmentation functions are smaller than 1%. After deriving new response matrices and efficiency corrections, the resulting systematic uncertainty in the fragmentation functions is found to be less than 0.5%. The tracking uncertainties shown in Figs. 2 and 3 include all the above explained track-related systematic uncertainties added in quadrature.

The correlations between the various systematic components in the two collision systems are considered when taking the ratios of $p + \text{Pb}$ to pp fragmentation functions. For the JES uncertainty, each source of uncertainty is classified as either correlated or uncorrelated between the two systems depending on its origin. The JER, unfolding and MC non-closure uncertainties are taken to be uncorrelated. For the tracking-related uncertainties the variation in the selection requirements, tracking in dense environments, secondary-track and fake-track rates, and parameterization of the efficiency corrections are taken as uncorrelated. The first three of these are conservatively considered as uncorrelated because the tracking system was augmented with the IBL and the tracking algorithm changed between the $p + \text{Pb}$ and pp data-taking periods. The uncertainties due to the track-to-particle matching and the inactive material in the MC samples are taken as correlated between $p + \text{Pb}$ and pp collisions. For the correlated uncertainties the ratios are re-evaluated applying the variation to both collision systems; the resulting variations of the ratios from their central values is used as the correlated systematic uncertainty. The total systematic uncertainties in the $R_{D(z)}$ and $R_{D(p_T)}$ distributions are shown in Figs. 4 and 5, respectively, for two p_T^{jet} intervals.

7. Results

The $D(z)$ and $D(p_T)$ distributions in both collision systems are shown in Figs. 6 and 7, respectively. Fig. 8 compares the $D(z)$ distribution in pp collisions at 5.02 TeV to the predictions from three event generators (PYTHIA6, PYTHIA8, and HERWIG++) using the parameter-value tunes and PDF sets described in Section 3 for the six p_T^{jet} intervals. The PYTHIA8 generator

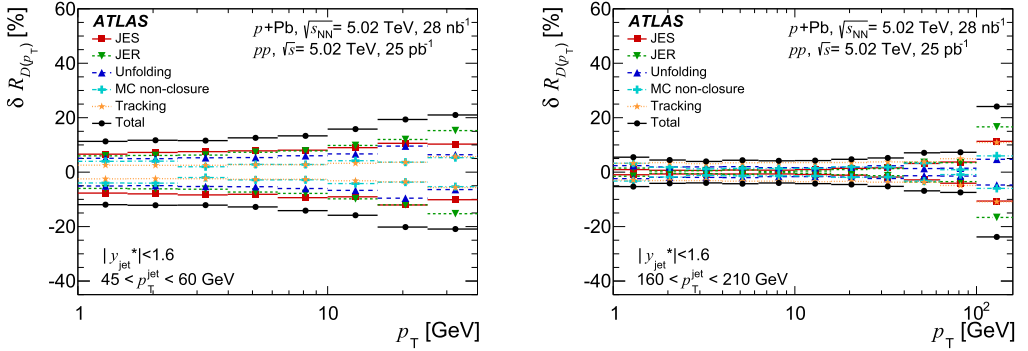


Fig. 5. Summary of the systematic uncertainties for $R_D(p_T)$ ratios, for jets in the 45–60 GeV p_T interval (left) and in the 160–210 GeV p_T interval (right). The systematic uncertainties due to JES, JER, unfolding, MC non-closure and tracking are shown along with the total systematic uncertainty from all sources.

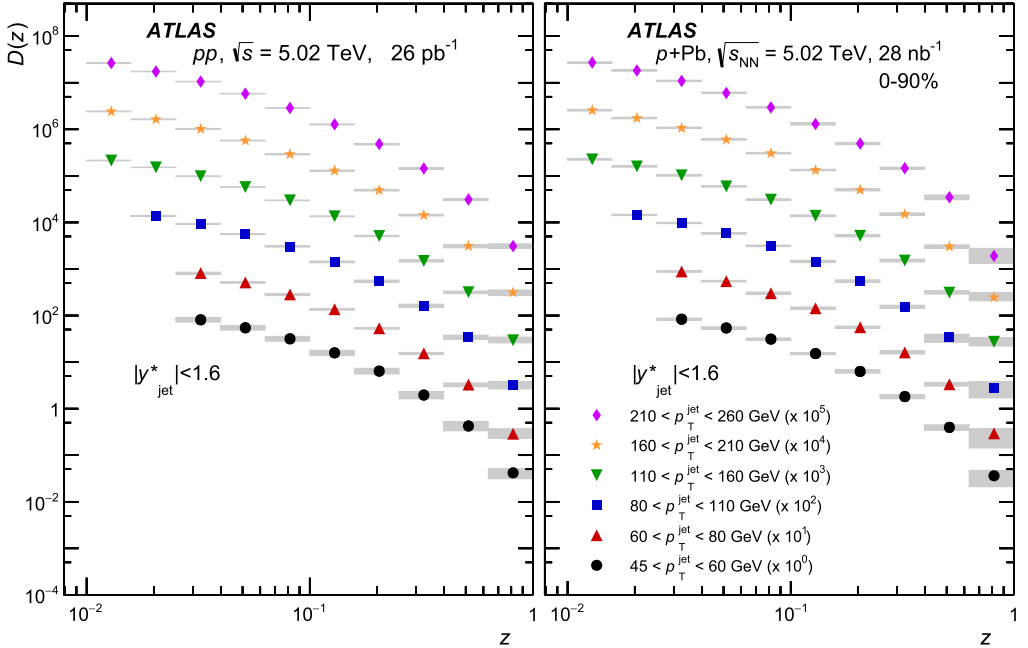


Fig. 6. Fragmentation functions as a function of the charged particle z in pp (left) and $p + \text{Pb}$ collisions (right) for the p_T^{jet} intervals used in this analysis. The fragmentation functions in both collision systems are offset by multiplicative factors for clarity as noted in the legend. The statistical uncertainties are shown as error bars and the systematic uncertainties are shown as shaded boxes. In many cases the statistical uncertainties are smaller than the marker size.

provides the best description of the data, generally agreeing within about 5 to 10% over the kinematic range used here. PYTHIA6 agrees within approximately 25% when compared to the data and HERWIG++ agrees within approximately 20% except for the highest z region, where there are some larger deviations. Similar agreement with PYTHIA6 and HERWIG++ generators with different tunes than used in this analysis was reported by ATLAS in the measurement of

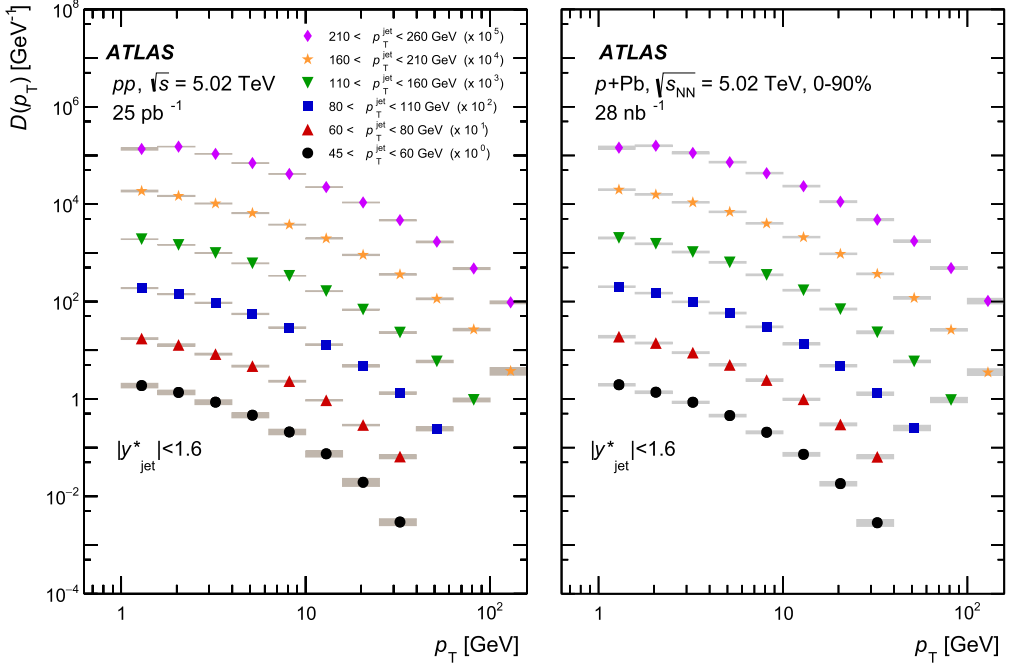


Fig. 7. Fragmentation functions as a function of the charged particle p_T in pp (left) and $p + \text{Pb}$ collisions (right) for the p_T^{jet} intervals used in this analysis. The fragmentation functions in both collision systems are offset by multiplicative factors for clarity as noted in the legend. The statistical uncertainties are shown as error bars and the systematic uncertainties are shown as shaded boxes. In many cases the statistical uncertainties are smaller than the marker size.

fragmentation functions in 7 TeV pp collisions [49]. The tunes of PYTHIA6 and PYTHIA8 used here include the results from that measurement.

Fig. 9 shows the pp fragmentation functions compared to two theoretical calculations. These predictions use a slightly different definition of z compared to the definition used in this measurement. This can introduce a difference between the fragmentation functions of approximately 1%. The calculation in Refs. [50,51] provides fragmentation functions with next-to-leading-order (NLO) accuracy as well as a resummation of logarithms in the jet cone size. The calculation in Ref. [52] is at NLO and uses the approximation that the jet cone is narrow. For the parton-to-charged-hadron fragmentation functions, both calculations use DSS07 fragmentation functions [53]. The uncertainties in the theoretical calculation are not estimated, including the uncertainty in DSS07, which is common to both calculations. The calculations are systematically higher than the data and generally agree within 20–30%. Larger deviations are observed at the low and high z regions. The DSS07 fragmentation functions have a minimum z of 0.05 and the calculations use extrapolated fragmentation functions in the region below $z = 0.05$.

Figs. 10 and 11 show the ratios of fragmentation functions in $p + \text{Pb}$ collisions to those in pp collisions, as a function of z and p_T respectively for p_T^{jet} from 45 to 260 GeV. Over the kinematic range selected here, the $R_{D(z)}$ and $R_{D(p_T)}$ distributions show deviations from unity of up to approximately 5% (up to 10% for 60–80 GeV jet selections) for $z < 0.1$ and $p_T < 10$ GeV. The deviations are larger than the reported systematic uncertainties by at most a couple of percent and always less than 1.5σ of the systematic uncertainties. At higher z and

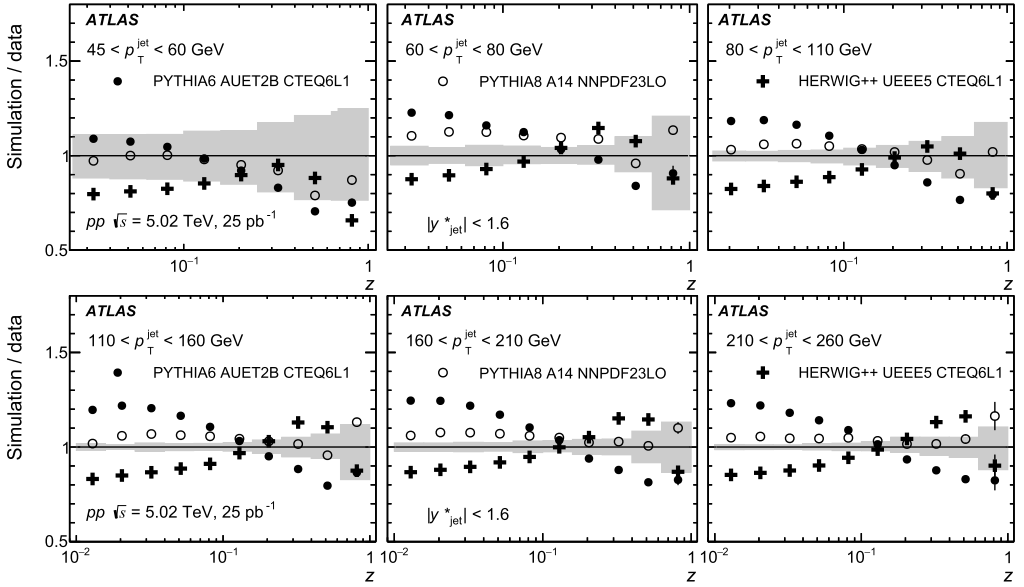


Fig. 8. Ratios of the particle-level $D(z)$ distributions from PYTHIA6, PYTHIA8, and HERWIG++ to the unfolded pp data for the six p_T^{jet} intervals used in this analysis. The statistical uncertainties are shown as error bars and the systematic uncertainties in the data are shown as the shaded region around unity. In many cases the statistical uncertainties are smaller than the marker size.

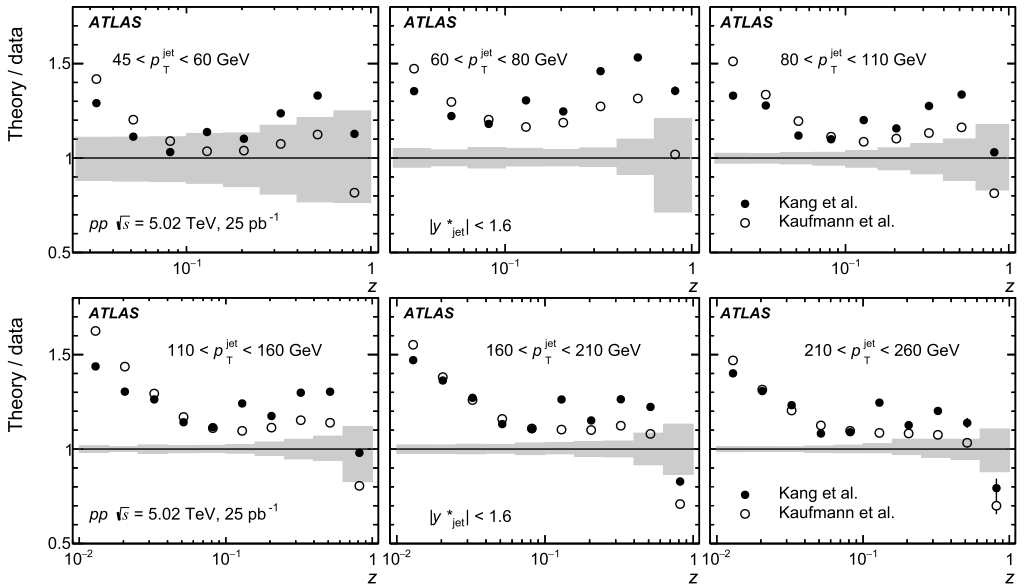


Fig. 9. Ratios of theoretical calculations from Refs. [50,51] (solid points) and Ref. [52] (open points) to the unfolded pp $D(z)$ distributions for the six p_T^{jet} intervals used in this analysis. The statistical uncertainties are shown as error bars and the systematic uncertainties in the data are shown as the shaded region around unity. The uncertainties in the theoretical calculations are not shown.

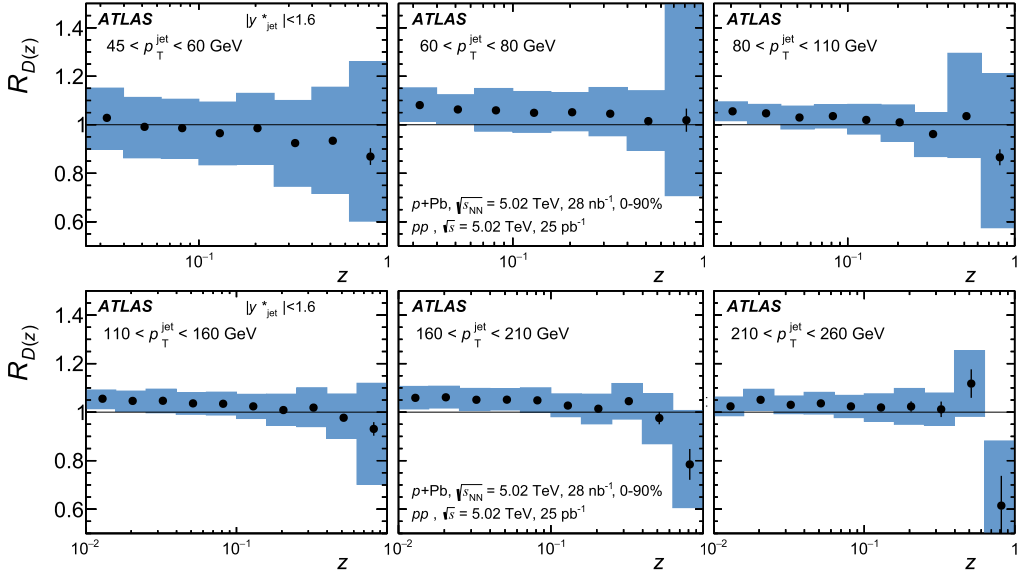


Fig. 10. Ratios of fragmentation functions as a function of the charged particle z in $p + \text{Pb}$ collisions to those in pp collisions for the six p_T^{jet} intervals. The statistical uncertainties are shown as error bars and the total systematic uncertainties are shown as shaded boxes.

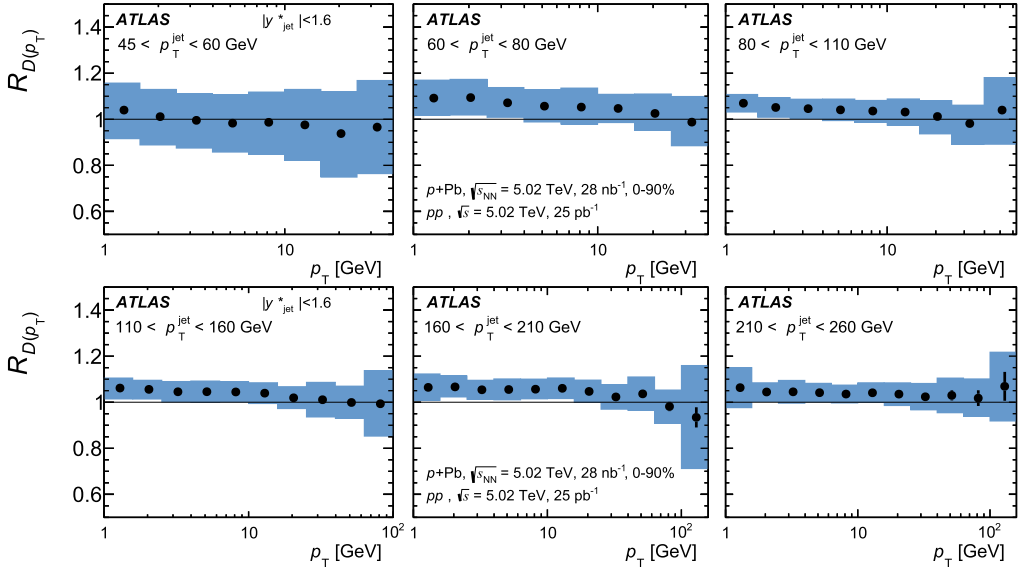


Fig. 11. Ratios of fragmentation functions as a function of the charged particle p_T in $p + \text{Pb}$ collisions to those in pp collisions for the six p_T^{jet} intervals. The statistical uncertainties are shown as error bars and the total systematic uncertainties are shown as shaded boxes.

p_T values the ratios are consistent with unity. At the highest z points for the 160–210 GeV and 210–260 GeV jet selections, deviations from unity of approximately 0.9σ and 1.3σ of combined statistical and systematic uncertainties, respectively, are observed. This is not observed in the $D(p_T)$ distributions. In most p_T^{jet} bins there is a slight decrease of the central values of $R_{D(z)}$ and $R_{D(p_T)}$ with increasing z and p_T ; however the size of the effect is smaller than the systematic uncertainties.

8. Summary

This paper presents the first measurement of the jet charged-particle fragmentation functions in a $p + A$ collisions system. The jet charged-particle fragmentation functions are reported for $|y_{\text{jet}}^*| < 1.6$ and p_T^{jet} from 45 to 260 GeV in $\sqrt{s_{\text{NN}}} = 5.02$ TeV $p + \text{Pb}$ and pp collisions with the ATLAS detector at the LHC. The measurement utilizes 28 nb^{-1} of $p + \text{Pb}$ data and 26 pb^{-1} of pp data. The pp fragmentation functions are compared to predictions from the PYTHIA6, PYTHIA8 and HERWIG++ generators. The generators show deviations from the pp data of up to approximately 25%, depending on z and the choice of generator. PYTHIA8 with the A14 tune and NNPDF23LO PDF set matches the data most closely. The pp $D(z)$ distributions are also compared to two theoretical calculations based on next-to-leading-order QCD and DSS07 fragmentation functions. The calculations are systematically higher than the data and agree generally within 20–30%, with larger deviations at small and large values of z . These measurements help constrain jet fragmentation in pp collisions. The ratios of fragmentation functions in $p + \text{Pb}$ collisions to those in pp collisions show no evidence for modification of jet fragmentation in $p + \text{Pb}$ collisions. This measurement provides new constraints on the modifications to jets in $p + \text{Pb}$ collisions at the LHC and is directly relevant to the current investigations into the properties of small collision systems. Finally, these measurements of jet fragmentation functions for different intervals of jet transverse momentum provide necessary baseline measurements for quantifying the effects of the quark-gluon plasma in $\text{Pb} + \text{Pb}$ collisions.

Acknowledgements

We thank CERN for the very successful operation of the LHC, as well as the support staff from our institutions without whom ATLAS could not be operated efficiently.

We acknowledge the support of ANPCyT, Argentina; YerPhI, Armenia; ARC, Australia; BMWFW and FWF, Austria; ANAS, Azerbaijan; SSTC, Belarus; CNPq and FAPESP, Brazil; NSERC, NRC and CFI, Canada; CERN; CONICYT, Chile; CAS, MOST and NSFC, China; COLCIENCIAS, Colombia; MSMT CR, MPO CR and VSC CR, Czech Republic; DNRF and DNSRC, Denmark; IN2P3-CNRS, CEA-DRF/IRFU, France; SRNSFG, Georgia; BMBF, HGF, and MPG, Germany; GSRT, Greece; RGC, Hong Kong SAR, China; ISF, I-CORE and Benoziyo Center, Israel; INFN, Italy; MEXT and JSPS, Japan; CNRST, Morocco; NWO, Netherlands; RCN, Norway; MNiSW and NCN, Poland; FCT, Portugal; MNE/IFA, Romania; MES of Russia and NRC KI, Russian Federation; JINR; MESTD, Serbia; MSSR, Slovakia; ARRS and MIZŠ, Slovenia; DST/NRF, South Africa; MINECO, Spain; SRC and Wallenberg Foundation, Sweden; SERI, SNSF and Cantons of Bern and Geneva, Switzerland; MOST, Taiwan; TAEK, Turkey; STFC, United Kingdom; DOE and NSF, United States of America. In addition, individual groups and members have received support from BCKDF, the Canada Council, CANARIE, CRC, Compute Canada, FQRNT, and the Ontario Innovation Trust, Canada; EPLANET, ERC, ERDF, FP7,

Horizon 2020 and Marie Skłodowska-Curie Actions, European Union; Investissements d’Avenir Labex and Idex, ANR, Région Auvergne and Fondation Partager le Savoir, France; DFG and AvH Foundation, Germany; Herakleitos, Thales and Aristeia programmes co-financed by EU-ESF and the Greek NSRF; BSF, GIF and Minerva, Israel; BRF, Norway; CERCA Programme Generalitat de Catalunya, Generalitat Valenciana, Spain; the Royal Society and Leverhulme Trust, United Kingdom. The crucial computing support from all WLCG partners is acknowledged gratefully, in particular from CERN, the ATLAS Tier-1 facilities at TRIUMF (Canada), NDGF (Denmark, Norway, Sweden), CC-IN2P3 (France), KIT/GridKA (Germany), INFN-CNAF (Italy), NL-T1 (Netherlands), PIC (Spain), ASGC (Taiwan), RAL (UK) and BNL (USA), the Tier-2 facilities worldwide and large non-WLCG resource providers. Major contributors of computing resources are listed in Ref. [54].

References

- [1] G. Roland, K. Safarik, P. Steinberg, Heavy-ion collisions at the LHC, *Prog. Part. Nucl. Phys.* 77 (2014) 70.
- [2] ATLAS Collaboration, Measurements of the nuclear modification factor for jets in Pb + Pb collisions at $\sqrt{s_{NN}} = 2.76$ TeV with the ATLAS detector, *Phys. Rev. Lett.* 114 (2015) 072302, arXiv:1411.2357 [hep-ex].
- [3] CMS Collaboration, Measurement of inclusive jet cross-sections in pp and PbPb collisions at $\sqrt{s_{NN}} = 2.76$ TeV, *Phys. Rev. C* 96 (1) (2017) 015202, arXiv:1609.05383 [nucl-ex].
- [4] ATLAS Collaboration, Measurement of inclusive jet charged-particle fragmentation functions in Pb + Pb collisions at $\sqrt{s_{NN}} = 2.76$ TeV with the ATLAS detector, *Phys. Lett. B* 739 (2014) 320, arXiv:1406.2979 [hep-ex].
- [5] ATLAS Collaboration, Measurement of internal structure of jets in Pb + Pb collisions at $\sqrt{s_{NN}} = 2.76$ TeV with the ATLAS detector at the LHC, *Eur. Phys. J. C* 77 (6) (2017) 379, arXiv:1702.00674 [hep-ex].
- [6] CMS Collaboration, Measurement of jet fragmentation in PbPb and pp collisions at $\sqrt{s_{NN}} = 2.76$ TeV, *Phys. Rev. C* 90 (2014) 024908, arXiv:1406.0932 [nucl-ex].
- [7] C. Salgado, J. Alvarez-Muniz, F. Arleo, N. Armesto, M. Botje, et al., Proton–nucleus collisions at the LHC: scientific opportunities and requirements, *J. Phys. G* 39 (2012) 015010, arXiv:1105.3919 [hep-ph].
- [8] Z.-B. Kang, I. Vitev, H. Xing, Effects of cold nuclear matter energy loss on inclusive jet production in p + A collisions at energies available at the BNL Relativistic Heavy Ion Collider and the CERN Large Hadron Collider, *Phys. Rev. C* 92 (2015) 054911, arXiv:1507.05987 [hep-ph].
- [9] ATLAS Collaboration, Centrality and rapidity dependence of inclusive jet production in $\sqrt{s_{NN}} = 5.02$ TeV proton–lead collisions with the ATLAS detector, *Phys. Lett. B* 748 (2015) 392, arXiv:1412.4092 [hep-ex].
- [10] ALICE Collaboration, Measurement of charged jet production cross sections and nuclear modification in p–Pb collisions at $\sqrt{s_{NN}} = 5.02$ TeV, *Phys. Lett. B* 749 (2015) 68, arXiv:1503.00681 [nucl-ex].
- [11] CMS Collaboration, Measurement of inclusive jet production and nuclear modifications in pPb collisions at $\sqrt{s_{NN}} = 5.02$ TeV, *Eur. Phys. J. C* 76 (2016) 372, arXiv:1601.02001 [nucl-ex].
- [12] A. Adare, et al., Centrality-dependent modification of jet-production rates in deuteron–gold collisions at $\sqrt{s_{NN}} = 200$ GeV, *Phys. Rev. Lett.* 116 (2016) 122301, arXiv:1509.04657 [nucl-ex].
- [13] CMS Collaboration, Charged-particle nuclear modification factors in PbPb and pPb collisions at $\sqrt{s_{NN}} = 5.02$ TeV, *J. High Energy Phys.* 04 (2017) 039, arXiv:1611.01664 [nucl-ex].
- [14] S. Chatrchyan, et al., Observation of long-range near-side angular correlations in proton–lead collisions at the LHC, *Phys. Lett. B* 718 (2013) 795, arXiv:1210.5482 [nucl-ex].
- [15] B. Abelev, et al., Long-range angular correlations on the near and away side in p–Pb collisions at $\sqrt{s_{NN}} = 5.02$ TeV, *Phys. Lett. B* 719 (2013) 29, arXiv:1212.2001 [nucl-ex].
- [16] G. Aad, et al., Observation of associated near-side and away-side long-range correlations in $\sqrt{s_{NN}} = 5.02$ TeV proton–lead collisions with the ATLAS detector, *Phys. Rev. Lett.* 110 (2013) 182302, arXiv:1212.5198 [hep-ex].
- [17] A. Adare, et al., Quadrupole anisotropy in dihadron azimuthal correlations in central d + Au collisions at $\sqrt{s_{NN}} = 200$ GeV, *Phys. Rev. Lett.* 111 (2013) 212301, arXiv:1303.1794 [nucl-ex].
- [18] A. Adare, et al., Nuclear modification of Ψ' , χ_c , and J/Ψ production in d + Au collisions at $\sqrt{s_{NN}} = 200$ GeV, *Phys. Rev. Lett.* 111 (2013) 202301, arXiv:1305.5516 [nucl-ex].
- [19] J. Adam, et al., Centrality dependence of $\psi(2S)$ suppression in p–Pb collisions at $\sqrt{s_{NN}} = 5.02$ TeV, *J. High Energy Phys.* 06 (2016) 050, arXiv:1603.02816 [nucl-ex].
- [20] A.M. Sirunyan, et al., Measurement of prompt and nonprompt J/ψ production in pp and pPb collisions at $\sqrt{s_{NN}} = 5.02$ TeV, *Eur. Phys. J. C* 77 (2017) 269, arXiv:1702.01462 [nucl-ex].

- [21] M. Aaboud, et al., Measurement of quarkonium production in proton–lead and proton–proton collisions at 5.02 TeV with the ATLAS detector, arXiv:1709.03089 [nucl-ex], 2017.
- [22] P. Bozek, W. Broniowski, Collective dynamics in high-energy proton–nucleus collisions, Phys. Rev. C 88 (2013) 014903, arXiv:1304.3044 [nucl-th].
- [23] K. Dusling, R. Venugopalan, Comparison of the color glass condensate to dihadron correlations in proton–proton and proton–nucleus collisions, Phys. Rev. D 87 (2013) 094034, arXiv:1302.7018 [hep-ph].
- [24] M. Cacciari, G.P. Salam, G. Soyez, The anti-kt jet clustering algorithm, J. High Energy Phys. 04 (2008) 063, arXiv:0802.1189 [hep-ph].
- [25] ATLAS Collaboration, The ATLAS experiment at the CERN Large Hadron Collider, J. Instrum. 3 (2008) S08003.
- [26] ATLAS Collaboration, ATLAS Insertable B-Layer Technical Design Report, ATLAS-TDR-19, <https://cds.cern.ch/record/1291633>, 2010;
ATLAS Collaboration, ATLAS Insertable B-Layer Technical Design Report Addendum, ATLAS-TDR-19-ADD-1, <https://cds.cern.ch/record/1451888>, 2012.
- [27] T. Sjöstrand, S. Mrenna, P.Z. Skands, PYTHIA 6.4 physics and manual, J. High Energy Phys. 05 (2006) 026, arXiv:hep-ph/0603175.
- [28] ATLAS Collaboration, ATLAS tunes of PYTHIA 6 and Pythia 8 for MC11, ATL-PHYS-PUB-2011-009, <https://cds.cern.ch/record/1363300>.
- [29] J. Pumplin, D. Stump, J. Huston, H. Lai, P.M. Nadolsky, et al., New generation of parton distributions with uncertainties from global QCD analysis, J. High Energy Phys. 07 (2002) 012, arXiv:hep-ph/0201195.
- [30] S. Agostinelli, et al., GEANT4: a simulation toolkit, Nucl. Instrum. Methods A 506 (2003) 250.
- [31] ATLAS Collaboration, The ATLAS simulation infrastructure, Eur. Phys. J. C 70 (2010) 823, arXiv:1005.4568 [physics.ins-det].
- [32] T. Sjöstrand, et al., An introduction to PYTHIA 8.2, Comput. Phys. Commun. 191 (2015) 159, arXiv:1410.3012 [hep-ph].
- [33] ATLAS Collaboration, ATLAS Run 1 Pythia8 tunes, ATLAS-PHYS-PUB-2014-021, <https://cds.cern.ch/record/1966419>.
- [34] R.D. Ball, et al., Parton distributions with LHC data, Nucl. Phys. B 867 (2013) 244, arXiv:1207.1303 [hep-ph].
- [35] M. Bahr, et al., HERWIG++ physics and manual, Eur. Phys. J. C 58 (2008) 639, arXiv:0803.0883 [hep-ph].
- [36] S. Gieseke, C. Rohr, A. Siodmok, Colour reconnections in HERWIG++, Eur. Phys. J. C 72 (2012) 2225, arXiv:1206.0041 [hep-ph].
- [37] ATLAS Collaboration, Jet energy measurement with the ATLAS detector in proton–proton collisions at $\sqrt{s} = 7$ TeV, Eur. Phys. J. C 73 (2013) 2304, arXiv:1112.6426 [hep-ex].
- [38] ATLAS Collaboration, Jet calibration and systematic uncertainties for jets reconstructed in the ATLAS detector at $\sqrt{s} = 13$ TeV, ATLAS-PHYS-PUB-2015-015, <https://cds.cern.ch/record/2037613>.
- [39] ATLAS Collaboration, Electron reconstruction and identification efficiency measurements with the ATLAS detector using the 2011 LHC proton–proton collision data, Eur. Phys. J. C 74 (2014) 2941, arXiv:1404.2240 [hep-ex].
- [40] G. D’Agostini, A Multidimensional unfolding method based on Bayes’ theorem, Nucl. Instrum. Methods A 362 (1995) 487.
- [41] T. Auye, Unfolding algorithms and tests using RooUnfold, arXiv:1105.1160 [physics.data-an], 2011.
- [42] ATLAS Collaboration, Jet energy scale and its uncertainty for jets reconstructed using the ATLAS heavy ion jet algorithm, ATLAS-CONF-2015-016, <https://cds.cern.ch/record/2008677>.
- [43] ATLAS Collaboration, Jet energy scale measurements and their systematic uncertainties in proton–proton collisions at $\sqrt{s} = 13$ TeV with the ATLAS detector, Phys. Rev. D 96 (7) (2017) 072002, arXiv:1703.09665 [hep-ex].
- [44] ATLAS Collaboration, Jet energy measurement and its systematic uncertainty in proton–proton collisions at $\sqrt{s} = 7$ TeV with the ATLAS detector, Eur. Phys. J. C 75 (2015) 17, arXiv:1406.0076 [hep-ex].
- [45] ATLAS Collaboration, Jet energy resolution in proton–proton collisions at $\sqrt{s} = 7$ TeV recorded in 2010 with the ATLAS detector, Eur. Phys. J. C 73 (2013) 2306, arXiv:1210.6210 [hep-ex].
- [46] ATLAS Collaboration, Data-driven determination of the energy scale and resolution of jets reconstructed in the ATLAS calorimeters using dijet and multijet events at $\sqrt{s} = 8$ TeV, ATLAS-CONF-2015-017, <https://cds.cern.ch/record/2008678>.
- [47] ATLAS Collaboration, Early inner detector tracking performance in the 2015 data at $\sqrt{s} = 13$ TeV, ATL-PHYS-PUB-2015-051, <https://cds.cern.ch/record/2110140>.
- [48] ATLAS Collaboration, Measurement of track reconstruction inefficiencies in the core of jets via pixel dE/dx with the ATLAS experiment using $\sqrt{s} = 13$ TeV pp collision data, ATL-PHYS-PUB-2016-007, <https://cds.cern.ch/record/2140460>.

- [49] ATLAS Collaboration, Measurement of the jet fragmentation function and transverse profile in proton–proton collisions at a center-of-mass energy of 7 TeV with the ATLAS detector, *Eur. Phys. J. C* 71 (2011) 1795, arXiv:1109.5816 [hep-ex].
- [50] Z.-B. Kang, F. Ringer, I. Vitev, Jet substructure using semi-inclusive jet functions in SCET, *J. High Energy Phys.* 11 (2016) 155, arXiv:1606.07063 [hep-ph].
- [51] Y.-T. Chien, Z.-B. Kang, F. Ringer, I. Vitev, H. Xing, Jet fragmentation functions in proton–proton collisions using soft-collinear effective theory, *J. High Energy Phys.* 05 (2016) 125, arXiv:1512.06851 [hep-ph].
- [52] T. Kaufmann, A. Mukherjee, W. Vogelsang, Hadron fragmentation inside jets in hadronic collisions, *Phys. Rev. D* 92 (2015) 054015, arXiv:1506.01415 [hep-ph].
- [53] D. de Florian, R. Sassot, M. Stratmann, Global analysis of fragmentation functions for protons and charged hadrons, *Phys. Rev. D* 76 (2007) 074033, arXiv:0707.1506 [hep-ph].
- [54] ATLAS Collaboration, ATLAS computing acknowledgements 2016–2017, ATL-GEN-PUB-2016-002, <https://cds.cern.ch/record/2202407>.

The ATLAS Collaboration

M. Aaboud^{137d}, G. Aad⁸⁸, B. Abbott¹¹⁵, J. Abdallah⁸, O. Abdinov^{12,*}, B. Abeloos¹¹⁹, S.H. Abidi¹⁶¹, O.S. AbouZeid¹³⁹, N.L. Abraham¹⁵¹, H. Abramowicz¹⁵⁵, H. Abreu¹⁵⁴, R. Abreu¹¹⁸, Y. Abulaiti^{148a,148b}, B.S. Acharya^{167a,167b,a}, S. Adachi¹⁵⁷, L. Adamczyk^{41a}, J. Adelman¹¹⁰, M. Adersberger¹⁰², T. Adye¹³³, A.A. Affolder¹³⁹, T. Agatonovic-Jovin¹⁴, C. Agheorghiesei^{28c}, J.A. Aguilar-Saavedra^{128a,128f}, S.P. Ahlen²⁴, F. Ahmadov^{68,b}, G. Aielli^{135a,135b}, S. Akatsuka⁷¹, H. Akerstedt^{148a,148b}, T.P.A. Åkesson⁸⁴, A.V. Akimov⁹⁸, G.L. Alberghi^{22a,22b}, J. Albert¹⁷², M.J. Alconada Verzini⁷⁴, M. Aleksa³², I.N. Aleksandrov⁶⁸, C. Alexa^{28b}, G. Alexander¹⁵⁵, T. Alexopoulos¹⁰, M. Alhroob¹¹⁵, B. Ali¹³⁰, M. Aliev^{76a,76b}, G. Alimonti^{94a}, J. Alison³³, S.P. Alkire³⁸, B.M.M. Allbrooke¹⁵¹, B.W. Allen¹¹⁸, P.P. Allport¹⁹, A. Aloisio^{106a,106b}, A. Alonso³⁹, F. Alonso⁷⁴, C. Alpigiani¹⁴⁰, A.A. Alshehri⁵⁶, M. Alstаты⁸⁸, B. Alvarez Gonzalez³², D. Álvarez Piqueras¹⁷⁰, M.G. Alvigi^{106a,106b}, B.T. Amadio¹⁶, Y. Amaral Coutinho^{26a}, C. Amelung²⁵, D. Amidei⁹², S.P. Amor Dos Santos^{128a,128c}, A. Amorim^{128a,128b}, S. Amoroso³², G. Amundsen²⁵, C. Anastopoulos¹⁴¹, L.S. Ancu⁵², N. Andari¹⁹, T. Andeen¹¹, C.F. Anders^{60b}, J.K. Anders⁷⁷, K.J. Anderson³³, A. Andreazza^{94a,94b}, V. Andrei^{60a}, S. Angelidakis⁹, I. Angelozzi¹⁰⁹, A. Angerami³⁸, A.V. Anisenkov^{111,c}, N. Anjos¹³, A. Annovi^{126a,126b}, C. Antel^{60a}, M. Antonelli⁵⁰, A. Antonov^{100,*}, D.J. Antrim¹⁶⁶, F. Anulli^{134a}, M. Aoki⁶⁹, L. Aperio Bella³², G. Arabidze⁹³, Y. Arai⁶⁹, J.P. Araque^{128a}, V. Araujo Ferraz^{26a}, A.T.H. Arce⁴⁸, R.E. Ardell⁸⁰, F.A. Arduh⁷⁴, J-F. Arguin⁹⁷, S. Argyropoulos⁶⁶, M. Arik^{20a}, A.J. Armbruster¹⁴⁵, L.J. Armitage⁷⁹, O. Arnaez¹⁶¹, H. Arnold⁵¹,

M. Arratia³⁰, O. Arslan²³, A. Artamonov⁹⁹, G. Artoni¹²², S. Artz⁸⁶,
 S. Asai¹⁵⁷, N. Asbah⁴⁵, A. Ashkenazi¹⁵⁵, L. Asquith¹⁵¹, K. Assamagan²⁷,
 R. Astalos^{146a}, M. Atkinson¹⁶⁹, N.B. Atlay¹⁴³, K. Augsten¹³⁰,
 G. Avolio³², B. Axen¹⁶, M.K. Ayoub¹¹⁹, G. Azuelos^{97,d}, A.E. Baas^{60a},
 M.J. Baca¹⁹, H. Bachacou¹³⁸, K. Bachas^{76a,76b}, M. Backes¹²²,
 M. Backhaus³², P. Bagiacci^{134a,134b}, P. Bagnaia^{134a,134b},
 H. Bahrasemani¹⁴⁴, J.T. Baines¹³³, M. Bajic³⁹, O.K. Baker¹⁷⁹,
 E.M. Baldin^{111,c}, P. Balek¹⁷⁵, T. Balestri¹⁵⁰, F. Balli¹³⁸, W.K. Balunas¹²⁴,
 E. Banas⁴², Sw. Banerjee^{176,e}, A.A.E. Bannoura¹⁷⁸, L. Barak³²,
 E.L. Barberio⁹¹, D. Barberis^{53a,53b}, M. Barbero⁸⁸, T. Barillari¹⁰³,
 M-S Barisits³², T. Barklow¹⁴⁵, N. Barlow³⁰, S.L. Barnes^{36c},
 B.M. Barnett¹³³, R.M. Barnett¹⁶, Z. Barnovska-Blenessy^{36a},
 A. Baroncelli^{136a}, G. Barone²⁵, A.J. Barr¹²², L. Barranco Navarro¹⁷⁰,
 F. Barreiro⁸⁵, J. Barreiro Guimarães da Costa^{35a}, R. Bartoldus¹⁴⁵,
 A.E. Barton⁷⁵, P. Bartos^{146a}, A. Basalae¹²⁵, A. Bassalat^{119,f},
 R.L. Bates⁵⁶, S.J. Batista¹⁶¹, J.R. Batley³⁰, M. Battaglia¹³⁹,
 M. Bauce^{134a,134b}, F. Bauer¹³⁸, H.S. Bawa^{145,g}, J.B. Beacham¹¹³,
 M.D. Beattie⁷⁵, T. Beau⁸³, P.H. Beauchemin¹⁶⁵, P. Bechtel²³,
 H.P. Beck^{18,h}, K. Becker¹²², M. Becker⁸⁶, M. Beckingham¹⁷³,
 C. Becot¹¹², A.J. Beddall^{20e}, A. Beddall^{20b}, V.A. Bednyakov⁶⁸,
 M. Bedognetti¹⁰⁹, C.P. Bee¹⁵⁰, T.A. Beermann³², M. Begalli^{26a},
 M. Begel²⁷, J.K. Behr⁴⁵, A.S. Bell⁸¹, G. Bella¹⁵⁵, L. Bellagamba^{22a},
 A. Bellerive³¹, M. Bellomo¹⁵⁴, K. Belotskiy¹⁰⁰, O. Beltramello³²,
 N.L. Belyaev¹⁰⁰, O. Benary^{155,*}, D. Benchekroun^{137a}, M. Bender¹⁰²,
 K. Bendtz^{148a,148b}, N. Benekos¹⁰, Y. Benhammou¹⁵⁵,
 E. Benhar Nocchioli¹⁷⁹, J. Benitez⁶⁶, D.P. Benjamin⁴⁸, M. Benoit⁵²,
 J.R. Bensinger²⁵, S. Bentvelsen¹⁰⁹, L. Beresford¹²², M. Beretta⁵⁰,
 D. Berge¹⁰⁹, E. Bergeaas Kuutmann¹⁶⁸, N. Berger⁵, J. Beringer¹⁶,
 S. Berlendis⁵⁸, N.R. Bernard⁸⁹, G. Bernardi⁸³, C. Bernius¹⁴⁵,
 F.U. Bernlochner²³, T. Berry⁸⁰, P. Berta¹³¹, C. Bertella^{35a},
 G. Bertoli^{148a,148b}, F. Bertolucci^{126a,126b}, I.A. Bertram⁷⁵, C. Bertsche⁴⁵,
 D. Bertsche¹¹⁵, G.J. Besjes³⁹, O. Bessidskaia Bylund^{148a,148b},
 M. Bessner⁴⁵, N. Besson¹³⁸, C. Betancourt⁵¹, A. Bethani⁸⁷, S. Bethke¹⁰³,
 A.J. Bevan⁷⁹, R.M. Bianchi¹²⁷, O. Biebel¹⁰², D. Biedermann¹⁷,
 R. Bielski⁸⁷, N.V. Biesuz^{126a,126b}, M. Biglietti^{136a},
 J. Bilbao De Mendizabal⁵², T.R.V. Billoud⁹⁷, H. Bilokon⁵⁰, M. Bindi⁵⁷,
 A. Bingul^{20b}, C. Bini^{134a,134b}, S. Biondi^{22a,22b}, T. Bisanz⁵⁷, C. Bittrich⁴⁷,

D.M. Bjergaard⁴⁸, C.W. Black¹⁵², J.E. Black¹⁴⁵, K.M. Black²⁴,
 D. Blackburn¹⁴⁰, R.E. Blair⁶, T. Blazek^{146a}, I. Bloch⁴⁵, C. Blocker²⁵,
 A. Blue⁵⁶, W. Blum^{86,*}, U. Blumenschein⁷⁹, S. Blunier^{34a},
 G.J. Bobbink¹⁰⁹, V.S. Bobrovnikov^{111,c}, S.S. Bocchetta⁸⁴, A. Bocci⁴⁸,
 C. Bock¹⁰², M. Boehler⁵¹, D. Boerner¹⁷⁸, D. Bogavac¹⁰²,
 A.G. Bogdanchikov¹¹¹, C. Bohm^{148a}, V. Boisvert⁸⁰, P. Bokan^{168,i},
 T. Bold^{41a}, A.S. Boldyrev¹⁰¹, A.E. Bolz^{60b}, M. Bomben⁸³, M. Bona⁷⁹,
 M. Boonekamp¹³⁸, A. Borisov¹³², G. Borissov⁷⁵, J. Bortfeldt³²,
 D. Bortoletto¹²², V. Bortolotto^{62a,62b,62c}, D. Boscherini^{22a}, M. Bosman¹³,
 J.D. Bossio Sola²⁹, J. Boudreau¹²⁷, J. Bouffard²,
 E.V. Bouhova-Thacker⁷⁵, D. Boumediene³⁷, C. Bourdarios¹¹⁹,
 S.K. Boutle⁵⁶, A. Boveia¹¹³, J. Boyd³², I.R. Boyko⁶⁸, J. Bracinik¹⁹,
 A. Brandt⁸, G. Brandt⁵⁷, O. Brandt^{60a}, U. Bratzler¹⁵⁸, B. Brau⁸⁹,
 J.E. Brau¹¹⁸, W.D. Breaden Madden⁵⁶, K. Brendlinger⁴⁵, A.J. Brennan⁹¹,
 L. Brenner¹⁰⁹, R. Brenner¹⁶⁸, S. Bressler¹⁷⁵, D.L. Briglin¹⁹,
 T.M. Bristow⁴⁹, D. Britton⁵⁶, D. Britzger⁴⁵, F.M. Brochu³⁰, I. Brock²³,
 R. Brock⁹³, G. Brooijmans³⁸, T. Brooks⁸⁰, W.K. Brooks^{34b},
 J. Brosamer¹⁶, E. Brost¹¹⁰, J.H. Broughton¹⁹,
 P.A. Bruckman de Renstrom⁴², D. Bruncko^{146b}, A. Bruni^{22a}, G. Bruni^{22a},
 L.S. Bruni¹⁰⁹, B.H. Brunt³⁰, M. Bruschi^{22a}, N. Bruscinò²³, P. Bryant³³,
 L. Bryngemark⁸⁴, T. Buanes¹⁵, Q. Buat¹⁴⁴, P. Buchholz¹⁴³,
 A.G. Buckley⁵⁶, I.A. Budagov⁶⁸, F. Buehrer⁵¹, M.K. Bugge¹²¹,
 O. Bulekov¹⁰⁰, D. Bullock⁸, H. Burckhart³², S. Burdin⁷⁷,
 C.D. Burgard⁵¹, A.M. Burger⁵, B. Burghgrave¹¹⁰, K. Burka⁴²,
 S. Burke¹³³, I. Burmeister⁴⁶, J.T.P. Burr¹²², E. Busato³⁷, D. Büscher⁵¹,
 V. Büscher⁸⁶, P. Bussey⁵⁶, J.M. Butler²⁴, C.M. Buttar⁵⁶,
 J.M. Butterworth⁸¹, P. Butti³², W. Buttinger²⁷, A. Buzatu^{35c},
 A.R. Buzykaev^{111,c}, S. Cabrera Urbán¹⁷⁰, D. Caforio¹³⁰,
 V.M. Cairo^{40a,40b}, O. Cakir^{4a}, N. Calace⁵², P. Calafiura¹⁶, A. Calandri⁸⁸,
 G. Calderini⁸³, P. Calfayan⁶⁴, G. Callea^{40a,40b}, L.P. Caloba^{26a},
 S. Calvente Lopez⁸⁵, D. Calvet³⁷, S. Calvet³⁷, T.P. Calvet⁸⁸,
 R. Camacho Toro³³, S. Camarda³², P. Camarri^{135a,135b}, D. Cameron¹²¹,
 R. Caminal Armadans¹⁶⁹, C. Camincher⁵⁸, S. Campana³²,
 M. Campanelli⁸¹, A. Camplani^{94a,94b}, A. Campoverde¹⁴³,
 V. Canale^{106a,106b}, M. Cano Bret^{36c}, J. Cantero¹¹⁶, T. Cao¹⁵⁵,
 M.D.M. Capeans Garrido³², I. Caprini^{28b}, M. Caprini^{28b}, M. Capua^{40a,40b},
 R.M. Carbone³⁸, R. Cardarelli^{135a}, F. Cardillo⁵¹, I. Carli¹³¹, T. Carli³²,

G. Carlini^{106a}, B.T. Carlson¹²⁷, L. Carminati^{94a,94b},
 R.M.D. Carney^{148a,148b}, S. Caron¹⁰⁸, E. Carquin^{34b}, S. Carrá^{94a,94b},
 G.D. Carrillo-Montoya³², J. Carvalho^{128a,128c}, D. Casadei¹⁹,
 M.P. Casado^{13,j}, M. Casolino¹³, D.W. Casper¹⁶⁶, R. Castelijin¹⁰⁹,
 A. Castelli¹⁰⁹, V. Castillo Gimenez¹⁷⁰, N.F. Castro^{128a,k}, A. Catinaccio³²,
 J.R. Catmore¹²¹, A. Cattai³², J. Caudron²³, V. Cavaliere¹⁶⁹,
 E. Cavallaro¹³, D. Cavalli^{94a}, M. Cavalli-Sforza¹³, V. Cavalinni^{126a,126b},
 E. Celebi^{20a}, F. Ceradini^{136a,136b}, L. Cerda Alberich¹⁷⁰, A.S. Cerqueira^{26b},
 A. Cerri¹⁵¹, L. Cerrito^{135a,135b}, F. Cerutti¹⁶, A. Cervelli¹⁸, S.A. Cetin^{20d},
 A. Chafaq^{137a}, D. Chakraborty¹¹⁰, S.K. Chan⁵⁹, W.S. Chan¹⁰⁹,
 Y.L. Chan^{62a}, P. Chang¹⁶⁹, J.D. Chapman³⁰, D.G. Charlton¹⁹,
 A. Chatterjee⁵², C.C. Chau¹⁶¹, C.A. Chavez Barajas¹⁵¹, S. Che¹¹³,
 S. Cheatham^{167a,167c}, A. Chegwidzen⁹³, S. Chekanov⁶,
 S.V. Chekulaev^{163a}, G.A. Chelkov^{68,l}, M.A. Chelstowska³², C. Chen⁶⁷,
 H. Chen²⁷, S. Chen^{35b}, S. Chen¹⁵⁷, X. Chen^{35c,m}, Y. Chen⁷⁰,
 H.C. Cheng⁹², H.J. Cheng^{35a}, Y. Cheng³³, A. Cheplakov⁶⁸,
 E. Cheremushkina¹³², R. Cherkaoui El Moursli^{137e}, V. Chernyatin^{27,*},
 E. Cheu⁷, L. Chevalier¹³⁸, V. Chiarella⁵⁰, G. Chiarelli^{126a,126b},
 G. Chiodini^{76a}, A.S. Chisholm³², A. Chitan^{28b}, Y.H. Chiu¹⁷²,
 M.V. Chizhov⁶⁸, K. Choi⁶⁴, A.R. Chomont³⁷, S. Chouridou¹⁵⁶,
 B.K.B. Chow¹⁰², V. Christodoulou⁸¹, D. Chromek-Burckhart³²,
 M.C. Chu^{62a}, J. Chudoba¹²⁹, A.J. Chuinard⁹⁰, J.J. Chwastowski⁴²,
 L. Chytka¹¹⁷, A.K. Ciftci^{4a}, D. Cinca⁴⁶, V. Cindro⁷⁸, I.A. Cioara²³,
 C. Ciocca^{22a,22b}, A. Ciocio¹⁶, F. Ciotto^{106a,106b}, Z.H. Citron¹⁷⁵,
 M. Citterio^{94a}, M. Ciubancan^{28b}, A. Clark⁵², B.L. Clark⁵⁹, M.R. Clark³⁸,
 P.J. Clark⁴⁹, R.N. Clarke¹⁶, C. Clement^{148a,148b}, Y. Coadou⁸⁸,
 M. Cobal^{167a,167c}, A. Coccaro⁵², J. Cochran⁶⁷, L. Colasurdo¹⁰⁸, B. Cole³⁸,
 A.P. Colijn¹⁰⁹, J. Collot⁵⁸, T. Colombo¹⁶⁶, P. Conde Muiño^{128a,128b},
 E. Coniavitis⁵¹, S.H. Connell^{147b}, I.A. Connelly⁸⁷, V. Consorti⁵¹,
 S. Constantinescu^{28b}, G. Conti³², F. Conventi^{106a,n}, M. Cooke¹⁶,
 B.D. Cooper⁸¹, A.M. Cooper-Sarkar¹²², F. Cormier¹⁷¹,
 K.J.R. Cormier¹⁶¹, M. Corradi^{134a,134b}, F. Corriveau^{90,o},
 A. Cortes-Gonzalez³², G. Cortiana¹⁰³, G. Costa^{94a}, M.J. Costa¹⁷⁰,
 D. Costanzo¹⁴¹, G. Cottin³⁰, G. Cowan⁸⁰, B.E. Cox⁸⁷, K. Cranmer¹¹²,
 S.J. Crawley⁵⁶, R.A. Creager¹²⁴, G. Cree³¹, S. Crépe-Renaudin⁵⁸,
 F. Crescioli⁸³, W.A. Cribbs^{148a,148b}, M. Crispin Ortuzar¹²²,
 M. Cristinziani²³, V. Croft¹⁰⁸, G. Crosetti^{40a,40b}, A. Cueto⁸⁵,

T. Cuhadar Donszelmann ¹⁴¹, A.R. Cukierman ¹⁴⁵, J. Cummings ¹⁷⁹,
 M. Curatolo ⁵⁰, J. Cúth ⁸⁶, H. Czirr ¹⁴³, P. Czodrowski ³², G. D’amen ^{22a,22b},
 S. D’Auria ⁵⁶, M. D’Onofrio ⁷⁷, M.J. Da Cunha Sargedas De Sousa ^{128a,128b},
 C. Da Via ⁸⁷, W. Dabrowski ^{41a}, T. Dado ^{146a}, T. Dai ⁹², O. Dale ¹⁵,
 F. Dallaire ⁹⁷, C. Dallapiccola ⁸⁹, M. Dam ³⁹, J.R. Dandoy ¹²⁴, N.P. Dang ⁵¹,
 A.C. Daniells ¹⁹, N.S. Dann ⁸⁷, M. Danninger ¹⁷¹, M. Dano Hoffmann ¹³⁸,
 V. Dao ¹⁵⁰, G. Darbo ^{53a}, S. Darmora ⁸, J. Dassoulas ³, A. Dattagupta ¹¹⁸,
 T. Daubney ⁴⁵, W. Davey ²³, C. David ⁴⁵, T. Davidek ¹³¹, M. Davies ¹⁵⁵,
 P. Davison ⁸¹, E. Dawe ⁹¹, I. Dawson ¹⁴¹, K. De ⁸, R. de Asmundis ^{106a},
 A. De Benedetti ¹¹⁵, S. De Castro ^{22a,22b}, S. De Cecco ⁸³, N. De Groot ¹⁰⁸,
 P. de Jong ¹⁰⁹, H. De la Torre ⁹³, F. De Lorenzi ⁶⁷, A. De Maria ⁵⁷,
 D. De Pedis ^{134a}, A. De Salvo ^{134a}, U. De Sanctis ^{135a,135b}, A. De Santo ¹⁵¹,
 K. De Vasconcelos Corga ⁸⁸, J.B. De Vivie De Regie ¹¹⁹,
 W.J. Dearnaley ⁷⁵, R. Debbe ²⁷, C. Debenedetti ¹³⁹, D.V. Dedovich ⁶⁸,
 N. Dehghanian ³, I. Deigaard ¹⁰⁹, M. Del Gaudio ^{40a,40b}, J. Del Peso ⁸⁵,
 T. Del Prete ^{126a,126b}, D. Delgove ¹¹⁹, F. Deliot ¹³⁸, C.M. Delitzsch ⁵²,
 A. Dell’Acqua ³², L. Dell’Asta ²⁴, M. Dell’Orso ^{126a,126b},
 M. Della Pietra ^{106a,106b}, D. della Volpe ⁵², M. Delmastro ⁵, C. Delporte ¹¹⁹,
 P.A. Delsart ⁵⁸, D.A. DeMarco ¹⁶¹, S. Demers ¹⁷⁹, M. Demichev ⁶⁸,
 A. Demilly ⁸³, S.P. Denisov ¹³², D. Denysiuk ¹³⁸, D. Derendarz ⁴²,
 J.E. Derkaoui ^{137d}, F. Derue ⁸³, P. Dervan ⁷⁷, K. Desch ²³, C. Deterre ⁴⁵,
 K. Dette ⁴⁶, P.O. Deviveiros ³², A. Dewhurst ¹³³, S. Dhaliwal ²⁵,
 A. Di Ciaccio ^{135a,135b}, L. Di Ciaccio ⁵, W.K. Di Clemente ¹²⁴,
 C. Di Donato ^{106a,106b}, A. Di Girolamo ³², B. Di Girolamo ³²,
 B. Di Micco ^{136a,136b}, R. Di Nardo ³², K.F. Di Petrillo ⁵⁹, A. Di Simone ⁵¹,
 R. Di Sipio ¹⁶¹, D. Di Valentino ³¹, C. Diaconu ⁸⁸, M. Diamond ¹⁶¹,
 F.A. Dias ⁴⁹, M.A. Diaz ^{34a}, E.B. Diehl ⁹², J. Dietrich ¹⁷, S. Díez Cornell ⁴⁵,
 A. Dimitrievska ¹⁴, J. Dingfelder ²³, P. Dita ^{28b}, S. Dita ^{28b}, F. Dittus ³²,
 F. Djama ⁸⁸, T. Djobava ^{54b}, J.I. Djuvsland ^{60a}, M.A.B. do Vale ^{26c},
 D. Dobos ³², M. Dobre ^{28b}, C. Doglioni ⁸⁴, J. Dolejsi ¹³¹, Z. Dolezal ¹³¹,
 M. Donadelli ^{26d}, S. Donati ^{126a,126b}, P. Dondero ^{123a,123b}, J. Donini ³⁷,
 J. Dopke ¹³³, A. Doria ^{106a}, M.T. Dova ⁷⁴, A.T. Doyle ⁵⁶, E. Drechsler ⁵⁷,
 M. Dris ¹⁰, Y. Du ^{36b}, J. Duarte-Campanerros ¹⁵⁵, E. Duchovni ¹⁷⁵,
 G. Duckeck ¹⁰², A. Ducourthial ⁸³, O.A. Ducu ^{97,p}, D. Duda ¹⁰⁹,
 A. Dudarev ³², A.Chr. Dudder ⁸⁶, E.M. Duffield ¹⁶, L. Dufлот ¹¹⁹,
 M. Dührssen ³², M. Dumancic ¹⁷⁵, A.E. Dumitriu ^{28b}, A.K. Duncan ⁵⁶,
 M. Dunford ^{60a}, H. Duran Yildiz ^{4a}, M. Düren ⁵⁵, A. Durglishvili ^{54b},

D. Duschinger⁴⁷, B. Dutta⁴⁵, M. Dyndal⁴⁵, C. Eckardt⁴⁵, K.M. Ecker¹⁰³,
 R.C. Edgar⁹², T. Eifert³², G. Eigen¹⁵, K. Einsweiler¹⁶, T. Ekelof¹⁶⁸,
 M. El Kacimi^{137c}, R. El Kosseifi⁸⁸, V. Ellajosyula⁸⁸, M. Ellert¹⁶⁸,
 S. Elles⁵, F. Ellinghaus¹⁷⁸, A.A. Elliot¹⁷², N. Ellis³², J. Elmsheuser²⁷,
 M. Elsing³², D. Emeliyanov¹³³, Y. Enari¹⁵⁷, O.C. Endner⁸⁶, J.S. Ennis¹⁷³,
 J. Erdmann⁴⁶, A. Ereditato¹⁸, G. Ernis¹⁷⁸, M. Ernst²⁷, S. Errede¹⁶⁹,
 E. Ertel⁸⁶, M. Escalier¹¹⁹, H. Esch⁴⁶, C. Escobar¹²⁷, B. Esposito⁵⁰,
 O. Estrada Pastor¹⁷⁰, A.I. Etienvre¹³⁸, E. Etzion¹⁵⁵, H. Evans⁶⁴,
 A. Ezhilov¹²⁵, M. Ezzi^{137e}, F. Fabbri^{22a,22b}, L. Fabbri^{22a,22b}, G. Facini³³,
 R.M. Fakhruddinov¹³², S. Falciano^{134a}, R.J. Falla⁸¹, J. Faltova³²,
 Y. Fang^{35a}, M. Fanti^{94a,94b}, A. Farbin⁸, A. Farilla^{136a}, C. Farina¹²⁷,
 E.M. Farina^{123a,123b}, T. Farooque⁹³, S. Farrell¹⁶, S.M. Farrington¹⁷³,
 P. Farthouat³², F. Fassi^{137e}, P. Fassnacht³², D. Fassouliotis⁹,
 M. Faucci Giannelli⁸⁰, A. Favareto^{53a,53b}, W.J. Fawcett¹²², L. Fayard¹¹⁹,
 O.L. Fedin^{125,q}, W. Fedorko¹⁷¹, S. Feigl¹²¹, L. Feligioni⁸⁸, C. Feng^{36b},
 E.J. Feng³², H. Feng⁹², A.B. Fenyuk¹³², L. Feremenga⁸,
 P. Fernandez Martinez¹⁷⁰, S. Fernandez Perez¹³, J. Ferrando⁴⁵,
 A. Ferrari¹⁶⁸, P. Ferrari¹⁰⁹, R. Ferrari^{123a}, D.E. Ferreira de Lima^{60b},
 A. Ferrer¹⁷⁰, D. Ferrere⁵², C. Ferretti⁹², F. Fiedler⁸⁶, A. Filipčič⁷⁸,
 M. Filipuzzi⁴⁵, F. Filthaut¹⁰⁸, M. Fincke-Keeler¹⁷², K.D. Finelli¹⁵²,
 M.C.N. Fiolhais^{128a,128c,r}, L. Fiorini¹⁷⁰, A. Fischer², C. Fischer¹³,
 J. Fischer¹⁷⁸, W.C. Fisher⁹³, N. Flaschel⁴⁵, I. Fleck¹⁴³, P. Fleischmann⁹²,
 R.R.M. Fletcher¹²⁴, T. Flick¹⁷⁸, B.M. Flierl¹⁰², L.R. Flores Castillo^{62a},
 M.J. Flowerdew¹⁰³, G.T. Forcolin⁸⁷, A. Formica¹³⁸, F.A. Förster¹³,
 A. Forti⁸⁷, A.G. Foster¹⁹, D. Fournier¹¹⁹, H. Fox⁷⁵, S. Fracchia¹⁴¹,
 P. Francavilla⁸³, M. Franchini^{22a,22b}, S. Franchino^{60a}, D. Francis³²,
 L. Franconi¹²¹, M. Franklin⁵⁹, M. Frate¹⁶⁶, M. Fraternali^{123a,123b},
 D. Freeborn⁸¹, S.M. Fressard-Batraneanu³², B. Freund⁹⁷,
 D. Froidevaux³², J.A. Frost¹²², C. Fukunaga¹⁵⁸, T. Fusayasu¹⁰⁴,
 J. Fuster¹⁷⁰, C. Gabaldon⁵⁸, O. Gabizon¹⁵⁴, A. Gabrielli^{22a,22b},
 A. Gabrielli¹⁶, G.P. Gach^{41a}, S. Gadatsch³², S. Gadomski⁸⁰,
 G. Gagliardi^{53a,53b}, L.G. Gagnon⁹⁷, P. Gagnon⁶⁴, C. Galea¹⁰⁸,
 B. Galhardo^{128a,128c}, E.J. Gallas¹²², B.J. Gallop¹³³, P. Gallus¹³⁰,
 G. Galster³⁹, K.K. Gan¹¹³, S. Ganguly³⁷, J. Gao^{36a}, Y. Gao⁷⁷,
 Y.S. Gao^{145,g}, F.M. Garay Walls⁴⁹, C. García¹⁷⁰, J.E. García Navarro¹⁷⁰,
 M. Garcia-Sciveres¹⁶, R.W. Gardner³³, N. Garelli¹⁴⁵, V. Garonne¹²¹,
 A. Gascon Bravo⁴⁵, K. Gasnikova⁴⁵, C. Gatti⁵⁰, A. Gaudiello^{53a,53b},

G. Gaudio ^{123a}, I.L. Gavrilenko ⁹⁸, C. Gay ¹⁷¹, G. Gaycken ²³, E.N. Gazis ¹⁰,
 C.N.P. Gee ¹³³, M. Geisen ⁸⁶, M.P. Geisler ^{60a}, K. Gellerstedt ^{148a,148b},
 C. Gemme ^{53a}, M.H. Genest ⁵⁸, C. Geng ^{36a,s}, S. Gentile ^{134a,134b},
 C. Gentsos ¹⁵⁶, S. George ⁸⁰, D. Gerbaudo ¹³, A. Gershon ¹⁵⁵,
 S. Ghasemi ¹⁴³, M. Ghneimat ²³, B. Giacobbe ^{22a}, S. Giagu ^{134a,134b},
 P. Giannetti ^{126a,126b}, S.M. Gibson ⁸⁰, M. Gignac ¹⁷¹, M. Gilchriese ¹⁶,
 D. Gillberg ³¹, G. Gilles ¹⁷⁸, D.M. Gingrich ^{3,d}, N. Giokaris ^{9,*},
 M.P. Giordani ^{167a,167c}, F.M. Giorgi ^{22a}, P.F. Giraud ¹³⁸, P. Giromini ⁵⁹,
 D. Giugni ^{94a}, F. Giuli ¹²², C. Giuliani ¹⁰³, M. Giulini ^{60b}, B.K. Gjelsten ¹²¹,
 S. Gkaitatzis ¹⁵⁶, I. Gkialas ^{9,t}, E.L. Gkoukousis ¹³⁹, L.K. Gladilin ¹⁰¹,
 C. Glasman ⁸⁵, J. Glatzer ¹³, P.C.F. Glaysher ⁴⁵, A. Glazov ⁴⁵,
 M. Goblirsch-Kolb ²⁵, J. Godlewski ⁴², S. Goldfarb ⁹¹, T. Golling ⁵²,
 D. Golubkov ¹³², A. Gomes ^{128a,128b,128d}, R. Gonçalves ^{128a},
 R. Goncalves Gama ^{26a}, J. Goncalves Pinto Firmino Da Costa ¹³⁸,
 G. Gonella ⁵¹, L. Gonella ¹⁹, A. Gongadze ⁶⁸, S. González de la Hoz ¹⁷⁰,
 S. Gonzalez-Sevilla ⁵², L. Goossens ³², P.A. Gorbounov ⁹⁹,
 H.A. Gordon ²⁷, I. Gorelov ¹⁰⁷, B. Gorini ³², E. Gorini ^{76a,76b}, A. Gorišek ⁷⁸,
 A.T. Goshaw ⁴⁸, C. Gössling ⁴⁶, M.I. Gostkin ⁶⁸, C.R. Goudet ¹¹⁹,
 D. Goujdami ^{137c}, A.G. Goussiou ¹⁴⁰, N. Govender ^{147b,u}, E. Gozani ¹⁵⁴,
 L. Graber ⁵⁷, I. Grabowska-Bold ^{41a}, P.O.J. Gradin ¹⁶⁸, J. Gramling ⁵²,
 E. Gramstad ¹²¹, S. Grancagnolo ¹⁷, V. Gratchev ¹²⁵, P.M. Gravila ^{28f},
 C. Gray ⁵⁶, H.M. Gray ³², Z.D. Greenwood ^{82,v}, C. Grefe ²³,
 K. Gregersen ⁸¹, I.M. Gregor ⁴⁵, P. Grenier ¹⁴⁵, K. Grevtsov ⁵, J. Griffiths ⁸,
 A.A. Grillo ¹³⁹, K. Grimm ⁷⁵, S. Grinstein ^{13,w}, Ph. Gris ³⁷, J.-F. Grivaz ¹¹⁹,
 S. Groh ⁸⁶, E. Gross ¹⁷⁵, J. Grosse-Knetter ⁵⁷, G.C. Grossi ⁸², Z.J. Grout ⁸¹,
 A. Grummer ¹⁰⁷, L. Guan ⁹², W. Guan ¹⁷⁶, J. Guenther ⁶⁵, F. Guescini ^{163a},
 D. Guest ¹⁶⁶, O. Gueta ¹⁵⁵, B. Gui ¹¹³, E. Guido ^{53a,53b}, T. Guillemain ⁵,
 S. Guindon ², U. Gul ⁵⁶, C. Gumpert ³², J. Guo ^{36c}, W. Guo ⁹², Y. Guo ^{36a},
 R. Gupta ⁴³, S. Gupta ¹²², G. Gustavino ^{134a,134b}, P. Gutierrez ¹¹⁵,
 N.G. Gutierrez Ortiz ⁸¹, C. Gutscheow ⁸¹, C. Guyot ¹³⁸, M.P. Guzik ^{41a},
 C. Gwenlan ¹²², C.B. Gwilliam ⁷⁷, A. Haas ¹¹², C. Haber ¹⁶,
 H.K. Hadavand ⁸, N. Haddad ^{137e}, A. Hadeef ⁸⁸, S. Hageböck ²³,
 M. Hagihara ¹⁶⁴, H. Hakobyan ^{180,*}, M. Haleem ⁴⁵, J. Haley ¹¹⁶,
 G. Halladjian ⁹³, G.D. Hallewell ⁸⁸, K. Hamacher ¹⁷⁸, P. Hamal ¹¹⁷,
 K. Hamano ¹⁷², A. Hamilton ^{147a}, G.N. Hamity ¹⁴¹, P.G. Hamnett ⁴⁵,
 L. Han ^{36a}, S. Han ^{35a}, K. Hanagaki ^{69,x}, K. Hanawa ¹⁵⁷, M. Hance ¹³⁹,
 B. Haney ¹²⁴, P. Hanke ^{60a}, J.B. Hansen ³⁹, J.D. Hansen ³⁹, M.C. Hansen ²³,

P.H. Hansen³⁹, K. Hara¹⁶⁴, A.S. Hard¹⁷⁶, T. Harenberg¹⁷⁸, F. Hariri¹¹⁹,
 S. Harkusha⁹⁵, R.D. Harrington⁴⁹, P.F. Harrison¹⁷³, N.M. Hartmann¹⁰²,
 M. Hasegawa⁷⁰, Y. Hasegawa¹⁴², A. Hasib⁴⁹, S. Hassani¹³⁸, S. Haug¹⁸,
 R. Hauser⁹³, L. Hauswald⁴⁷, L.B. Havener³⁸, M. Havranek¹³⁰,
 C.M. Hawkes¹⁹, R.J. Hawkings³², D. Hayakawa¹⁵⁹, D. Hayden⁹³,
 C.P. Hays¹²², J.M. Hays⁷⁹, H.S. Hayward⁷⁷, S.J. Haywood¹³³,
 S.J. Head¹⁹, T. Heck⁸⁶, V. Hedberg⁸⁴, L. Heelan⁸, K.K. Heidegger⁵¹,
 S. Heim⁴⁵, T. Heim¹⁶, B. Heinemann^{45,y}, J.J. Heinrich¹⁰², L. Heinrich¹¹²,
 C. Heinz⁵⁵, J. Hejbal¹²⁹, L. Helary³², A. Held¹⁷¹, S. Hellman^{148a,148b},
 C. Hensens³², J. Henderson¹²², R.C.W. Henderson⁷⁵, Y. Heng¹⁷⁶,
 S. Henkelmann¹⁷¹, A.M. Henriques Correia³², S. Henrot-Versille¹¹⁹,
 G.H. Herbert¹⁷, H. Herde²⁵, V. Herget¹⁷⁷, Y. Hernández Jiménez^{147c},
 G. Herten⁵¹, R. Hertenberger¹⁰², L. Hervas³², T.C. Herwig¹²⁴,
 G.G. Hesketh⁸¹, N.P. Hessey^{163a}, J.W. Hetherly⁴³, S. Higashino⁶⁹,
 E. Higón-Rodríguez¹⁷⁰, E. Hill¹⁷², J.C. Hill³⁰, K.H. Hiller⁴⁵,
 S.J. Hillier¹⁹, I. Hinchliffe¹⁶, M. Hirose⁵¹, D. Hirschbuehl¹⁷⁸, B. Hiti⁷⁸,
 O. Hladik¹²⁹, X. Hoad⁴⁹, J. Hobbs¹⁵⁰, N. Hod^{163a}, M.C. Hodgkinson¹⁴¹,
 P. Hodgson¹⁴¹, A. Hoecker³², M.R. Hoefkamp¹⁰⁷, F. Hoenig¹⁰²,
 D. Hohn²³, T.R. Holmes¹⁶, M. Homann⁴⁶, S. Honda¹⁶⁴, T. Honda⁶⁹,
 T.M. Hong¹²⁷, B.H. Hooberman¹⁶⁹, W.H. Hopkins¹¹⁸, Y. Horii¹⁰⁵,
 A.J. Horton¹⁴⁴, J.-Y. Hostachy⁵⁸, S. Hou¹⁵³, A. Hoummada^{137a},
 J. Howarth⁴⁵, J. Hoya⁷⁴, M. Hrabovsky¹¹⁷, I. Hristova¹⁷, J. Hrivnac¹¹⁹,
 T. Hryn'ova⁵, A. Hrynevich⁹⁶, P.J. Hsu⁶³, S.-C. Hsu¹⁴⁰, Q. Hu^{36a},
 S. Hu^{36c}, Y. Huang^{35a}, Z. Hubacek¹³⁰, F. Hubaut⁸⁸, F. Huegging²³,
 T.B. Huffman¹²², E.W. Hughes³⁸, G. Hughes⁷⁵, M. Huhtinen³²,
 P. Huo¹⁵⁰, N. Huseynov^{68,b}, J. Huston⁹³, J. Huth⁵⁹, G. Iacobucci⁵²,
 G. Iakovidis²⁷, I. Ibragimov¹⁴³, L. Iconomidou-Fayard¹¹⁹, Z. Idrissi^{137e},
 P. Iengo³², O. Igonkina^{109,z}, T. Iizawa¹⁷⁴, Y. Ikegami⁶⁹, M. Ikeno⁶⁹,
 Y. Ilchenko^{11,aa}, D. Iliadis¹⁵⁶, N. Ilic¹⁴⁵, G. Introzzi^{123a,123b}, P. Ioannou^{9,*},
 M. Iodice^{136a}, K. Iordanidou³⁸, V. Ippolito⁵⁹, M.F. Isacson¹⁶⁸,
 N. Ishijima¹²⁰, M. Ishino¹⁵⁷, M. Ishitsuka¹⁵⁹, C. Issever¹²², S. Istin^{20a},
 F. Ito¹⁶⁴, J.M. Iturbe Ponce⁸⁷, R. Iuppa^{162a,162b}, H. Iwasaki⁶⁹, J.M. Izen⁴⁴,
 V. Izzo^{106a}, S. Jabbar³, P. Jackson¹, V. Jain², K.B. Jakobi⁸⁶, K. Jakobs⁵¹,
 S. Jakobsen³², T. Jakoubek¹²⁹, D.O. Jamin¹¹⁶, D.K. Jana⁸², R. Jansky⁶⁵,
 J. Janssen²³, M. Janus⁵⁷, P.A. Janus^{41a}, G. Jarlskog⁸⁴, N. Javadov^{68,b},
 T. Javůrek⁵¹, M. Javurkova⁵¹, F. Jeanneau¹³⁸, L. Jeanty¹⁶,
 J. Jejelava^{54a,ab}, A. Jelinskas¹⁷³, P. Jenni^{51,ac}, C. Jeske¹⁷³, S. Jézéquel⁵,

H. Ji ¹⁷⁶, J. Jia ¹⁵⁰, H. Jiang ⁶⁷, Y. Jiang ^{36a}, Z. Jiang ¹⁴⁵, S. Jiggins ⁸¹,
 J. Jimenez Pena ¹⁷⁰, S. Jin ^{35a}, A. Jinaru ^{28b}, O. Jinnouchi ¹⁵⁹, H. Jivan ^{147c},
 P. Johansson ¹⁴¹, K.A. Johns ⁷, C.A. Johnson ⁶⁴, W.J. Johnson ¹⁴⁰,
 K. Jon-And ^{148a,148b}, R.W.L. Jones ⁷⁵, S.D. Jones ¹⁵¹, S. Jones ⁷,
 T.J. Jones ⁷⁷, J. Jongmanns ^{60a}, P.M. Jorge ^{128a,128b}, J. Jovicevic ^{163a},
 X. Ju ¹⁷⁶, A. Juste Rozas ^{13,w}, M.K. Köhler ¹⁷⁵, A. Kaczmarska ⁴²,
 M. Kado ¹¹⁹, H. Kagan ¹¹³, M. Kagan ¹⁴⁵, S.J. Kahn ⁸⁸, T. Kaji ¹⁷⁴,
 E. Kajomovitz ⁴⁸, C.W. Kalderon ⁸⁴, A. Kaluza ⁸⁶, S. Kama ⁴³,
 A. Kamenshchikov ¹³², N. Kanaya ¹⁵⁷, S. Kaneti ³⁰, L. Kanjir ⁷⁸,
 V.A. Kantserov ¹⁰⁰, J. Kanzaki ⁶⁹, B. Kaplan ¹¹², L.S. Kaplan ¹⁷⁶,
 D. Kar ^{147c}, K. Karakostas ¹⁰, N. Karastathis ¹⁰, M.J. Kareem ⁵⁷,
 E. Karentzos ¹⁰, S.N. Karpov ⁶⁸, Z.M. Karpova ⁶⁸, K. Karthik ¹¹²,
 V. Kartvelishvili ⁷⁵, A.N. Karyukhin ¹³², K. Kasahara ¹⁶⁴, L. Kashif ¹⁷⁶,
 R.D. Kass ¹¹³, A. Kastanas ¹⁴⁹, Y. Kataoka ¹⁵⁷, C. Kato ¹⁵⁷, A. Katre ⁵²,
 J. Katzy ⁴⁵, K. Kawade ¹⁰⁵, K. Kawagoe ⁷³, T. Kawamoto ¹⁵⁷,
 G. Kawamura ⁵⁷, E.F. Kay ⁷⁷, V.F. Kazanin ^{111,c}, R. Keeler ¹⁷², R. Kehoe ⁴³,
 J.S. Keller ⁴⁵, J.J. Kempster ⁸⁰, H. Keoshkerian ¹⁶¹, O. Kepka ¹²⁹,
 B.P. Kerševan ⁷⁸, S. Kersten ¹⁷⁸, R.A. Keyes ⁹⁰, M. Khader ¹⁶⁹,
 F. Khalil-zada ¹², A. Khanov ¹¹⁶, A.G. Kharlamov ^{111,c}, T. Kharlamova ^{111,c},
 A. Khodinov ¹⁶⁰, T.J. Khoo ⁵², V. Khovanskiy ^{99,*}, E. Khramov ⁶⁸,
 J. Khubua ^{54b,ad}, S. Kido ⁷⁰, C.R. Kilby ⁸⁰, H.Y. Kim ⁸, S.H. Kim ¹⁶⁴,
 Y.K. Kim ³³, N. Kimura ¹⁵⁶, O.M. Kind ¹⁷, B.T. King ⁷⁷, D. Kirchmeier ⁴⁷,
 J. Kirk ¹³³, A.E. Kiryunin ¹⁰³, T. Kishimoto ¹⁵⁷, D. Kisielewska ^{41a},
 K. Kiuchi ¹⁶⁴, O. Kivernyk ⁵, E. Kladiva ^{146b}, T. Klapdor-Kleingrothaus ⁵¹,
 M.H. Klein ³⁸, M. Klein ⁷⁷, U. Klein ⁷⁷, K. Kleinknecht ⁸⁶, P. Klimek ¹¹⁰,
 A. Klimentov ²⁷, R. Klingenberg ⁴⁶, T. Klingl ²³, T. Klioutchnikova ³²,
 E.-E. Kluge ^{60a}, P. Kluit ¹⁰⁹, S. Kluth ¹⁰³, J. Knapik ⁴², E. Kneringer ⁶⁵,
 E.B.F.G. Knoop ⁸⁸, A. Knue ¹⁰³, A. Kobayashi ¹⁵⁷, D. Kobayashi ¹⁵⁹,
 T. Kobayashi ¹⁵⁷, M. Kobel ⁴⁷, M. Kocian ¹⁴⁵, P. Kodys ¹³¹, T. Koffas ³¹,
 E. Koffeman ¹⁰⁹, N.M. Köhler ¹⁰³, T. Koi ¹⁴⁵, M. Kolb ^{60b}, I. Koletsou ⁵,
 A.A. Komar ^{98,*}, Y. Komori ¹⁵⁷, T. Kondo ⁶⁹, N. Kondrashova ^{36c},
 K. Köneke ⁵¹, A.C. König ¹⁰⁸, T. Kono ^{69,ae}, R. Konoplich ^{112,af},
 N. Konstantinidis ⁸¹, R. Kopeliansky ⁶⁴, S. Koperny ^{41a}, A.K. Kopp ⁵¹,
 K. Korcyl ⁴², K. Kordas ¹⁵⁶, A. Korn ⁸¹, A.A. Korol ^{111,c}, I. Korolkov ¹³,
 E.V. Korolkova ¹⁴¹, O. Kortner ¹⁰³, S. Kortner ¹⁰³, T. Kosek ¹³¹,
 V.V. Kostyukhin ²³, A. Kotwal ⁴⁸, A. Koulouris ¹⁰,
 A. Kourkoumeli-Charalampidi ^{123a,123b}, C. Kourkoumelis ⁹, E. Kourlitis ¹⁴¹,

V. Kouskoura²⁷, A.B. Kowalewska⁴², R. Kowalewski¹⁷²,
 T.Z. Kowalski^{41a}, C. Kozakai¹⁵⁷, W. Kozanecki¹³⁸, A.S. Kozhin¹³²,
 V.A. Kramarenko¹⁰¹, G. Kramberger⁷⁸, D. Krasnopevtsev¹⁰⁰,
 M.W. Krasny⁸³, A. Krasznahorkay³², D. Krauss¹⁰³, A. Kravchenko²⁷,
 J.A. Kremer^{41a}, M. Kretz^{60c}, J. Kretzschmar⁷⁷, K. Kreutzfeldt⁵⁵,
 P. Krieger¹⁶¹, K. Krizka³³, K. Kroeninger⁴⁶, H. Kroha¹⁰³, J. Kroll¹²⁹,
 J. Kroll¹²⁴, J. Kroseberg²³, J. Krstic¹⁴, U. Kruchonak⁶⁸, H. Krüger²³,
 N. Krumnack⁶⁷, M.C. Kruse⁴⁸, M. Kruskal²⁴, T. Kubota⁹¹, H. Kucuk⁸¹,
 S. Kuday^{4b}, J.T. Kuechler¹⁷⁸, S. Kuehn³², A. Kugel^{60c}, F. Kuger¹⁷⁷,
 T. Kuhl⁴⁵, V. Kukhtin⁶⁸, R. Kukla⁸⁸, Y. Kulchitsky⁹⁵, S. Kuleshov^{34b},
 Y.P. Kulinich¹⁶⁹, M. Kuna^{134a,134b}, T. Kunigo⁷¹, A. Kupco¹²⁹,
 O. Kuprash¹⁵⁵, H. Kurashige⁷⁰, L.L. Kurchaninov^{163a}, Y.A. Kurochkin⁹⁵,
 M.G. Kurth^{35a}, V. Kus¹²⁹, E.S. Kuwertz¹⁷², M. Kuze¹⁵⁹, J. Kvita¹¹⁷,
 T. Kwan¹⁷², D. Kyriazopoulos¹⁴¹, A. La Rosa¹⁰³,
 J.L. La Rosa Navarro^{26d}, L. La Rotonda^{40a,40b}, C. Lacasta¹⁷⁰,
 F. Lacava^{134a,134b}, J. Lacey⁴⁵, H. Lacker¹⁷, D. Lacour⁸³, E. Ladygin⁶⁸,
 R. Lafaye⁵, B. Laforge⁸³, T. Lagouri¹⁷⁹, S. Lai⁵⁷, S. Lammers⁶⁴,
 W. Lampl⁷, E. Lançon²⁷, U. Landgraf⁵¹, M.P.J. Landon⁷⁹,
 M.C. Lanfermann⁵², V.S. Lang^{60a}, J.C. Lange¹³, A.J. Lankford¹⁶⁶,
 F. Lanni²⁷, K. Lantzsch²³, A. Lanza^{123a}, A. Lapertosa^{53a,53b}, S. Laplace⁸³,
 J.F. Laporte¹³⁸, T. Lari^{94a}, F. Lasagni Manghi^{22a,22b}, M. Lassnig³²,
 P. Laurelli⁵⁰, W. Lavrijsen¹⁶, A.T. Law¹³⁹, P. Laycock⁷⁷, T. Lazovich⁵⁹,
 M. Lazzaroni^{94a,94b}, B. Le⁹¹, O. Le Dortz⁸³, E. Le Guirriec⁸⁸,
 E.P. Le Quilleuc¹³⁸, M. LeBlanc¹⁷², T. LeCompte⁶, F. Ledroit-Guillon⁵⁸,
 C.A. Lee²⁷, G.R. Lee^{133,ag}, S.C. Lee¹⁵³, L. Lee⁵⁹, B. Lefebvre⁹⁰,
 G. Lefebvre⁸³, M. Lefebvre¹⁷², F. Legger¹⁰², C. Leggett¹⁶, A. Lehan⁷⁷,
 G. Lehmann Miotto³², X. Lei⁷, W.A. Leight⁴⁵, M.A.L. Leite^{26d},
 R. Leitner¹³¹, D. Lellouch¹⁷⁵, B. Lemmer⁵⁷, K.J.C. Leney⁸¹, T. Lenz²³,
 B. Lenzi³², R. Leone⁷, S. Leone^{126a,126b}, C. Leonidopoulos⁴⁹,
 G. Lerner¹⁵¹, C. Leroy⁹⁷, A.A.J. Lesage¹³⁸, C.G. Lester³⁰,
 M. Levchenko¹²⁵, J. Levêque⁵, D. Levin⁹², L.J. Levinson¹⁷⁵, M. Levy¹⁹,
 D. Lewis⁷⁹, B. Li^{36a,s}, Changqiao Li^{36a}, H. Li¹⁵⁰, L. Li^{36c}, Q. Li^{35a},
 S. Li⁴⁸, X. Li^{36c}, Y. Li¹⁴³, Z. Liang^{35a}, B. Liberti^{135a}, A. Liblong¹⁶¹,
 K. Lie^{62c}, J. Liebal²³, W. Liebig¹⁵, A. Limosani¹⁵², S.C. Lin^{153,ah},
 T.H. Lin⁸⁶, B.E. Lindquist¹⁵⁰, A.E. Lioni⁵², E. Lipeles¹²⁴,
 A. Lipniacka¹⁵, M. Lisovyi^{60b}, T.M. Liss^{169,ai}, A. Lister¹⁷¹,
 A.M. Litke¹³⁹, B. Liu^{153,aj}, H. Liu⁹², H. Liu²⁷, J.K.K. Liu¹²², J. Liu^{36b},

J.B. Liu ^{36a}, K. Liu ⁸⁸, L. Liu ¹⁶⁹, M. Liu ^{36a}, Y.L. Liu ^{36a}, Y. Liu ^{36a},
 M. Livan ^{123a,123b}, A. Lleres ⁵⁸, J. Llorente Merino ^{35a}, S.L. Lloyd ⁷⁹,
 C.Y. Lo ^{62b}, F. Lo Sterzo ¹⁵³, E.M. Lobodzinska ⁴⁵, P. Loch ⁷,
 F.K. Loebinger ⁸⁷, K.M. Loew ²⁵, A. Loginov ^{179,*}, T. Lohse ¹⁷,
 K. Lohwasser ⁴⁵, M. Lokajicek ¹²⁹, B.A. Long ²⁴, J.D. Long ¹⁶⁹,
 R.E. Long ⁷⁵, L. Longo ^{76a,76b}, K.A. Looper ¹¹³, J.A. Lopez ^{34b},
 D. Lopez Mateos ⁵⁹, I. Lopez Paz ¹³, A. Lopez Solis ⁸³, J. Lorenz ¹⁰²,
 N. Lorenzo Martinez ⁵, M. Losada ²¹, P.J. Lösel ¹⁰², X. Lou ^{35a},
 A. Lounis ¹¹⁹, J. Love ⁶, P.A. Love ⁷⁵, H. Lu ^{62a}, N. Lu ⁹², Y.J. Lu ⁶³,
 H.J. Lubatti ¹⁴⁰, C. Luci ^{134a,134b}, A. Lucotte ⁵⁸, C. Luedtke ⁵¹,
 F. Luehring ⁶⁴, W. Lukas ⁶⁵, L. Luminari ^{134a}, O. Lundberg ^{148a,148b},
 B. Lund-Jensen ¹⁴⁹, P.M. Luzi ⁸³, D. Lynn ²⁷, R. Lysak ¹²⁹, E. Lytken ⁸⁴,
 V. Lyubushkin ⁶⁸, H. Ma ²⁷, L.L. Ma ^{36b}, Y. Ma ^{36b}, G. Maccarrone ⁵⁰,
 A. Macchiolo ¹⁰³, C.M. Macdonald ¹⁴¹, B. Maček ⁷⁸,
 J. Machado Miguens ^{124,128b}, D. Madaffari ⁸⁸, R. Madar ³⁷,
 H.J. Maddocks ¹⁶⁸, W.F. Mader ⁴⁷, A. Madsen ⁴⁵, J. Maeda ⁷⁰,
 S. Maeland ¹⁵, T. Maeno ²⁷, A.S. Maevskiy ¹⁰¹, E. Magradze ⁵⁷,
 J. Mahlstedt ¹⁰⁹, C. Maiani ¹¹⁹, C. Maidantchik ^{26a}, A.A. Maier ¹⁰³,
 T. Maier ¹⁰², A. Maio ^{128a,128b,128d}, S. Majewski ¹¹⁸, Y. Makida ⁶⁹,
 N. Makovec ¹¹⁹, B. Malaescu ⁸³, Pa. Malecki ⁴², V.P. Maleev ¹²⁵,
 F. Malek ⁵⁸, U. Mallik ⁶⁶, D. Malon ⁶, C. Malone ³⁰, S. Maltezos ¹⁰,
 S. Malyukov ³², J. Mamuzic ¹⁷⁰, G. Mancini ⁵⁰, L. Mandelli ^{94a},
 I. Mandić ⁷⁸, J. Maneira ^{128a,128b}, L. Manhaes de Andrade Filho ^{26b},
 J. Manjarres Ramos ^{163b}, A. Mann ¹⁰², A. Manousos ³², B. Mansoulie ¹³⁸,
 J.D. Mansour ^{35a}, R. Mantifel ⁹⁰, M. Mantoani ⁵⁷, S. Manzoni ^{94a,94b},
 L. Mapelli ³², G. Marceca ²⁹, L. March ⁵², L. Marchese ¹²², G. Marchiori ⁸³,
 M. Marcisovsky ¹²⁹, M. Marjanovic ³⁷, D.E. Marley ⁹², F. Marroquim ^{26a},
 S.P. Marsden ⁸⁷, Z. Marshall ¹⁶, M.U.F. Martensson ¹⁶⁸, S. Marti-Garcia ¹⁷⁰,
 C.B. Martin ¹¹³, T.A. Martin ¹⁷³, V.J. Martin ⁴⁹, B. Martin dit Latour ¹⁵,
 M. Martinez ^{13,w}, V.I. Martinez Outschoorn ¹⁶⁹, S. Martin-Haugh ¹³³,
 V.S. Martoiu ^{28b}, A.C. Martyniuk ⁸¹, A. Marzin ³², L. Masetti ⁸⁶,
 T. Mashimo ¹⁵⁷, R. Mashinistov ⁹⁸, J. Masik ⁸⁷, A.L. Maslennikov ^{111,c},
 L. Massa ^{135a,135b}, P. Mastrandrea ⁵, A. Mastroberardino ^{40a,40b},
 T. Masubuchi ¹⁵⁷, P. Mättig ¹⁷⁸, J. Maurer ^{28b}, S.J. Maxfield ⁷⁷,
 D.A. Maximov ^{111,c}, R. Mazini ¹⁵³, I. Maznas ¹⁵⁶, S.M. Mazza ^{94a,94b},
 N.C. Mc Fadden ¹⁰⁷, G. Mc Goldrick ¹⁶¹, S.P. Mc Kee ⁹², A. McCarn ⁹²,
 R.L. McCarthy ¹⁵⁰, T.G. McCarthy ¹⁰³, L.I. McClymont ⁸¹,

E.F. McDonald⁹¹, J.A. McFayden⁸¹, G. Mchedlidze⁵⁷, S.J. McMahon¹³³,
 P.C. McNamara⁹¹, R.A. McPherson^{172,o}, S. Meehan¹⁴⁰, T.J. Megy⁵¹,
 S. Mehlhase¹⁰², A. Mehta⁷⁷, T. Meideck⁵⁸, K. Meier^{60a}, C. Meineck¹⁰²,
 B. Meirose⁴⁴, D. Melini^{170,ak}, B.R. Mellado Garcia^{147c}, M. Melo^{146a},
 F. Meloni¹⁸, S.B. Menary⁸⁷, L. Meng⁷⁷, X.T. Meng⁹²,
 A. Mengarelli^{22a,22b}, S. Menke¹⁰³, E. Meoni^{40a,40b}, S. Mergelmeyer¹⁷,
 P. Mermod⁵², L. Merola^{106a,106b}, C. Meroni^{94a}, F.S. Merritt³³,
 A. Messina^{134a,134b}, J. Metcalfe⁶, A.S. Mete¹⁶⁶, C. Meyer¹²⁴,
 J-P. Meyer¹³⁸, J. Meyer¹⁰⁹, H. Meyer Zu Theenhausen^{60a}, F. Miano¹⁵¹,
 R.P. Middleton¹³³, S. Miglioranzi^{53a,53b}, L. Mijović⁴⁹, G. Mikenberg¹⁷⁵,
 M. Mikestikova¹²⁹, M. Mikuž⁷⁸, M. Milesi⁹¹, A. Milic²⁷, D.W. Miller³³,
 C. Mills⁴⁹, A. Milov¹⁷⁵, D.A. Milstead^{148a,148b}, A.A. Minaenko¹³²,
 Y. Minami¹⁵⁷, I.A. Minashvili⁶⁸, A.I. Mincer¹¹², B. Mindur^{41a},
 M. Mineev⁶⁸, Y. Minegishi¹⁵⁷, Y. Ming¹⁷⁶, L.M. Mir¹³, K.P. Mistry¹²⁴,
 T. Mitani¹⁷⁴, J. Mitrevski¹⁰², V.A. Mitsou¹⁷⁰, A. Miucci¹⁸,
 P.S. Miyagawa¹⁴¹, A. Mizukami⁶⁹, J.U. Mjörnmark⁸⁴,
 M. Mlynarikova¹³¹, T. Moa^{148a,148b}, K. Mochizuki⁹⁷, P. Mogg⁵¹,
 S. Mohapatra³⁸, S. Molander^{148a,148b}, R. Moles-Valls²³, R. Monden⁷¹,
 M.C. Mondragon⁹³, K. Mönig⁴⁵, J. Monk³⁹, E. Monnier⁸⁸,
 A. Montalbano¹⁵⁰, J. Montejo Berlingen³², F. Monticelli⁷⁴,
 S. Monzani^{94a,94b}, R.W. Moore³, N. Morange¹¹⁹, D. Moreno²¹,
 M. Moreno Llácer⁵⁷, P. Morettini^{53a}, S. Morgenstern³², D. Mori¹⁴⁴,
 T. Mori¹⁵⁷, M. Morii⁵⁹, M. Morinaga¹⁵⁷, V. Morisbak¹²¹,
 A.K. Morley¹⁵², G. Mornacchi³², J.D. Morris⁷⁹, L. Morvaj¹⁵⁰,
 P. Moschovakos¹⁰, M. Mosidze^{54b}, H.J. Moss¹⁴¹, J. Moss^{145,al},
 K. Motohashi¹⁵⁹, R. Mount¹⁴⁵, E. Mountricha²⁷, E.J.W. Moyses⁸⁹,
 S. Muanza⁸⁸, R.D. Mudd¹⁹, F. Mueller¹⁰³, J. Mueller¹²⁷,
 R.S.P. Mueller¹⁰², D. Muenstermann⁷⁵, P. Mullen⁵⁶, G.A. Mullier¹⁸,
 F.J. Munoz Sanchez⁸⁷, W.J. Murray^{173,133}, H. Musheghyan³²,
 M. Muškinja⁷⁸, A.G. Myagkov^{132,am}, M. Myska¹³⁰, B.P. Nachman¹⁶,
 O. Nackenhorst⁵², K. Nagai¹²², R. Nagai^{69,ae}, K. Nagano⁶⁹,
 Y. Nagasaka⁶¹, K. Nagata¹⁶⁴, M. Nagel⁵¹, E. Nagy⁸⁸, A.M. Nairz³²,
 Y. Nakahama¹⁰⁵, K. Nakamura⁶⁹, T. Nakamura¹⁵⁷, I. Nakano¹¹⁴,
 R.F. Naranjo Garcia⁴⁵, R. Narayan¹¹, D.I. Narrias Villar^{60a},
 I. Naryshkin¹²⁵, T. Naumann⁴⁵, G. Navarro²¹, R. Nayyar⁷, H.A. Neal⁹²,
 P.Yu. Nechaeva⁹⁸, T.J. Neep¹³⁸, A. Negri^{123a,123b}, M. Negrini^{22a},
 S. Nektarijevic¹⁰⁸, C. Nellist¹¹⁹, A. Nelson¹⁶⁶, M.E. Nelson¹²²,

S. Nemecek ¹²⁹, P. Nemethy ¹¹², A.A. Nepomuceno ^{26a}, M. Nessi ^{32,an},
 M.S. Neubauer ¹⁶⁹, M. Neumann ¹⁷⁸, P.R. Newman ¹⁹, T.Y. Ng ^{62c},
 T. Nguyen Manh ⁹⁷, R.B. Nickerson ¹²², R. Nicolaidou ¹³⁸, J. Nielsen ¹³⁹,
 V. Nikolaenko ^{132,am}, I. Nikolic-Audit ⁸³, K. Nikolopoulos ¹⁹,
 J.K. Nilsen ¹²¹, P. Nilsson ²⁷, Y. Ninomiya ¹⁵⁷, A. Nisati ^{134a}, N. Nishu ^{35c},
 R. Nisius ¹⁰³, T. Nobe ¹⁵⁷, Y. Noguchi ⁷¹, M. Nomachi ¹²⁰, I. Nomidis ³¹,
 M.A. Nomura ²⁷, T. Nooney ⁷⁹, M. Nordberg ³², N. Norjoharuddeen ¹²²,
 O. Novgorodova ⁴⁷, S. Nowak ¹⁰³, M. Nozaki ⁶⁹, L. Nozka ¹¹⁷,
 K. Ntekas ¹⁶⁶, E. Nurse ⁸¹, F. Nuti ⁹¹, K. O’connor ²⁵, D.C. O’Neil ¹⁴⁴,
 A.A. O’Rourke ⁴⁵, V. O’Shea ⁵⁶, F.G. Oakham ^{31,d}, H. Oberlack ¹⁰³,
 T. Obermann ²³, J. Ocariz ⁸³, A. Ochi ⁷⁰, I. Ochoa ³⁸, J.P. Ochoa-Ricoux ^{34a},
 S. Oda ⁷³, S. Odaka ⁶⁹, H. Ogren ⁶⁴, A. Oh ⁸⁷, S.H. Oh ⁴⁸, C.C. Ohm ¹⁶,
 H. Ohman ¹⁶⁸, H. Oide ^{53a,53b}, H. Okawa ¹⁶⁴, Y. Okumura ¹⁵⁷,
 T. Okuyama ⁶⁹, A. Olariu ^{28b}, L.F. Oleiro Seabra ^{128a}, S.A. Olivares Pino ⁴⁹,
 D. Oliveira Damazio ²⁷, A. Olszewski ⁴², J. Olszowska ⁴²,
 A. Onofre ^{128a,128e}, K. Onogi ¹⁰⁵, P.U.E. Onyisi ^{11,aa}, M.J. Oreglia ³³,
 Y. Oren ¹⁵⁵, D. Orestano ^{136a,136b}, N. Orlando ^{62b}, R.S. Orr ¹⁶¹,
 B. Osculati ^{53a,53b,*}, R. Ospanov ⁸⁷, G. Otero y Garzon ²⁹, H. Otono ⁷³,
 M. Ouchrif ^{137d}, F. Ould-Saada ¹²¹, A. Ouraou ¹³⁸, K.P. Oussoren ¹⁰⁹,
 Q. Ouyang ^{35a}, M. Owen ⁵⁶, R.E. Owen ¹⁹, V.E. Ozcan ^{20a}, N. Ozturk ⁸,
 K. Pachal ¹⁴⁴, A. Pacheco Pages ¹³, L. Pacheco Rodriguez ¹³⁸,
 C. Padilla Aranda ¹³, S. Pagan Griso ¹⁶, M. Paganini ¹⁷⁹, F. Paige ²⁷,
 P. Pais ⁸⁹, G. Palacino ⁶⁴, S. Palazzo ^{40a,40b}, S. Palestini ³², M. Palka ^{41b},
 D. Pallin ³⁷, E.St. Panagiotopoulou ¹⁰, I. Panagoulas ¹⁰, C.E. Pandini ⁸³,
 J.G. Panduro Vazquez ⁸⁰, P. Pani ³², S. Panitkin ²⁷, D. Pantea ^{28b},
 L. Paolozzi ⁵², Th.D. Papadopoulou ¹⁰, K. Papageorgiou ^{9,t},
 A. Paramonov ⁶, D. Paredes Hernandez ¹⁷⁹, A.J. Parker ⁷⁵, M.A. Parker ³⁰,
 K.A. Parker ⁴⁵, F. Parodi ^{53a,53b}, J.A. Parsons ³⁸, U. Parzefall ⁵¹,
 V.R. Pascuzzi ¹⁶¹, J.M. Pasner ¹³⁹, E. Pasqualucci ^{134a}, S. Passaggio ^{53a},
 Fr. Pastore ⁸⁰, S. Pataraiia ¹⁷⁸, J.R. Pater ⁸⁷, T. Pauly ³², J. Pearce ¹⁷²,
 B. Pearson ¹⁰³, S. Pedraza Lopez ¹⁷⁰, R. Pedro ^{128a,128b},
 S.V. Peleganchuk ^{111,c}, O. Penc ¹²⁹, C. Peng ^{35a}, H. Peng ^{36a}, J. Penwell ⁶⁴,
 B.S. Peralva ^{26b}, M.M. Perego ¹³⁸, D.V. Perepelitsa ²⁷, L. Perini ^{94a,94b},
 H. Pernegger ³², S. Perrella ^{106a,106b}, R. Peschke ⁴⁵, V.D. Peshekhonov ^{68,*},
 K. Peters ⁴⁵, R.F.Y. Peters ⁸⁷, B.A. Petersen ³², T.C. Petersen ³⁹, E. Petit ⁵⁸,
 A. Petridis ¹, C. Petridou ¹⁵⁶, P. Petroff ¹¹⁹, E. Petrolo ^{134a}, M. Petrov ¹²²,
 F. Petrucci ^{136a,136b}, N.E. Pettersson ⁸⁹, A. Peyaud ¹³⁸, R. Pezoa ^{34b},

F.H. Phillips⁹³, P.W. Phillips¹³³, G. Piacquadio¹⁵⁰, E. Pianori¹⁷³,
 A. Picazio⁸⁹, E. Piccaro⁷⁹, M.A. Pickering¹²², R. Piegaia²⁹,
 J.E. Pilcher³³, A.D. Pilkington⁸⁷, A.W.J. Pin⁸⁷, M. Pinamonti^{135a,135b},
 J.L. Pinfold³, H. Pirumov⁴⁵, M. Pitt¹⁷⁵, L. Plazak^{146a}, M.-A. Pleier²⁷,
 V. Pleskot⁸⁶, E. Plotnikova⁶⁸, D. Pluth⁶⁷, P. Podberezko¹¹¹,
 R. Poettgen^{148a,148b}, R. Poggi^{123a,123b}, L. Poggioli¹¹⁹, D. Pohl²³,
 G. Polesello^{123a}, A. Poley⁴⁵, A. Policicchio^{40a,40b}, R. Polifka³²,
 A. Polini^{22a}, C.S. Pollard⁵⁶, V. Polychronakos²⁷, K. Pommès³²,
 D. Ponomarenko¹⁰⁰, L. Pontecorvo^{134a}, B.G. Pope⁹³, G.A. Popeneciu^{28d},
 A. Poppleton³², S. Pospisil¹³⁰, K. Potamianos¹⁶, I.N. Potrap⁶⁸,
 C.J. Potter³⁰, G. Poulard³², J. Poveda³², M.E. Pozo Astigarraga³²,
 P. Pralavorio⁸⁸, A. Pranko¹⁶, S. Prell⁶⁷, D. Price⁸⁷, L.E. Price⁶,
 M. Primavera^{76a}, S. Prince⁹⁰, N. Proklova¹⁰⁰, K. Prokofiev^{62c},
 F. Prokoshin^{34b}, S. Protopopescu²⁷, J. Proudfoot⁶, M. Przybycien^{41a},
 D. Puddu^{136a,136b}, A. Puri¹⁶⁹, P. Puzo¹¹⁹, J. Qian⁹², G. Qin⁵⁶, Y. Qin⁸⁷,
 A. Quadt⁵⁷, M. Queitsch-Maitland⁴⁵, D. Quilty⁵⁶, S. Raddum¹²¹,
 V. Radeka²⁷, V. Radescu¹²², S.K. Radhakrishnan¹⁵⁰, P. Radloff¹¹⁸,
 P. Rados⁹¹, F. Ragusa^{94a,94b}, G. Rahal¹⁸¹, J.A. Raine⁸⁷, S. Rajagopalan²⁷,
 C. Rangel-Smith¹⁶⁸, T. Rashid¹¹⁹, M.G. Ratti^{94a,94b}, D.M. Rauch⁴⁵,
 F. Rauscher¹⁰², S. Rave⁸⁶, T. Ravenscroft⁵⁶, I. Ravinovich¹⁷⁵,
 J.H. Rawling⁸⁷, M. Raymond³², A.L. Read¹²¹, N.P. Readioff⁷⁷,
 M. Reale^{76a,76b}, D.M. Rebuzzi^{123a,123b}, A. Redelbach¹⁷⁷, G. Redlinger²⁷,
 R. Reece¹³⁹, R.G. Reed^{147c}, K. Reeves⁴⁴, L. Rehnisch¹⁷, J. Reichert¹²⁴,
 A. Reiss⁸⁶, C. Rembser³², H. Ren^{35a}, M. Rescigno^{134a}, S. Resconi^{94a},
 E.D. Resseguie¹²⁴, S. Rettie¹⁷¹, E. Reynolds¹⁹, O.L. Rezanova^{111,c},
 P. Reznicek¹³¹, R. Rezvani⁹⁷, R. Richter¹⁰³, S. Richter⁸¹,
 E. Richter-Was^{41b}, O. Ricken²³, M. Ridel⁸³, P. Rieck¹⁰³, C.J. Riegel¹⁷⁸,
 J. Rieger⁵⁷, O. Rifki¹¹⁵, M. Rijssenbeek¹⁵⁰, A. Rimoldi^{123a,123b},
 M. Rimoldi¹⁸, L. Rinaldi^{22a}, B. Ristić⁵², E. Ritsch³², I. Riu¹³,
 F. Rizatdinova¹¹⁶, E. Rizvi⁷⁹, C. Rizzi¹³, R.T. Roberts⁸⁷,
 S.H. Robertson^{90,o}, A. Robichaud-Veronneau⁹⁰, D. Robinson³⁰,
 J.E.M. Robinson⁴⁵, A. Robson⁵⁶, E. Rocco⁸⁶, C. Roda^{126a,126b},
 Y. Rodina^{88,ao}, S. Rodriguez Bosca¹⁷⁰, A. Rodriguez Perez¹³,
 D. Rodriguez Rodriguez¹⁷⁰, S. Roe³², C.S. Rogan⁵⁹, O. Røhne¹²¹,
 J. Roloff⁵⁹, A. Romaniouk¹⁰⁰, M. Romano^{22a,22b}, S.M. Romano Saez³⁷,
 E. Romero Adam¹⁷⁰, N. Rompotis⁷⁷, M. Ronzani⁵¹, L. Roos⁸³,
 S. Rosati^{134a}, K. Rosbach⁵¹, P. Rose¹³⁹, N.-A. Rosien⁵⁷,

V. Rossetti^{148a,148b}, E. Rossi^{106a,106b}, L.P. Rossi^{53a}, J.H.N. Rosten³⁰,
R. Rosten¹⁴⁰, M. Rotaru^{28b}, I. Roth¹⁷⁵, J. Rothberg¹⁴⁰, D. Rousseau¹¹⁹,
A. Rozanov⁸⁸, Y. Rozen¹⁵⁴, X. Ruan^{147c}, F. Rubbo¹⁴⁵, F. Rühr⁵¹,
A. Ruiz-Martinez³¹, Z. Rurikova⁵¹, N.A. Rusakovich⁶⁸, H.L. Russell¹⁴⁰,
J.P. Rutherford⁷, N. Ruthmann³², Y.F. Ryabov¹²⁵, M. Rybar¹⁶⁹,
G. Rybkin¹¹⁹, S. Ryu⁶, A. Ryzhov¹³², G.F. Rzehorz⁵⁷, A.F. Saavedra¹⁵²,
G. Sabato¹⁰⁹, S. Sacerdoti²⁹, H.F-W. Sadrozinski¹³⁹, R. Sadykov⁶⁸,
F. Safai Tehrani^{134a}, P. Saha¹¹⁰, M. Sahinsoy^{60a}, M. Saimpert⁴⁵,
M. Saito¹⁵⁷, T. Saito¹⁵⁷, H. Sakamoto¹⁵⁷, Y. Sakurai¹⁷⁴,
G. Salamanna^{136a,136b}, J.E. Salazar Loyola^{34b}, D. Salek¹⁰⁹,
P.H. Sales De Bruin¹⁶⁸, D. Salihagic¹⁰³, A. Salnikov¹⁴⁵, J. Salt¹⁷⁰,
D. Salvatore^{40a,40b}, F. Salvatore¹⁵¹, A. Salvucci^{62a,62b,62c}, A. Salzburger³²,
D. Sammel⁵¹, D. Sampsonidis¹⁵⁶, D. Sampsonidou¹⁵⁶, J. Sánchez¹⁷⁰,
V. Sanchez Martinez¹⁷⁰, A. Sanchez Pineda^{167a,167c}, H. Sandaker¹²¹,
R.L. Sandbach⁷⁹, C.O. Sander⁴⁵, M. Sandhoff¹⁷⁸, C. Sandoval²¹,
D.P.C. Sankey¹³³, M. Sannino^{53a,53b}, A. Sansoni⁵⁰, C. Santoni³⁷,
R. Santonico^{135a,135b}, H. Santos^{128a}, I. Santoyo Castillo¹⁵¹, K. Sapp¹²⁷,
A. Sapronov⁶⁸, J.G. Saraiva^{128a,128d}, B. Sarrazin²³, O. Sasaki⁶⁹,
K. Sato¹⁶⁴, E. Sauvan⁵, G. Savage⁸⁰, P. Savard^{161,d}, N. Savic¹⁰³,
C. Sawyer¹³³, L. Sawyer^{82,v}, J. Saxon³³, C. Sbarra^{22a}, A. Sbrizzi^{22a,22b},
T. Scanlon⁸¹, D.A. Scannicchio¹⁶⁶, M. Scarcella¹⁵², V. Scarfone^{40a,40b},
J. Schaarschmidt¹⁴⁰, P. Schacht¹⁰³, B.M. Schachtner¹⁰², D. Schaefer³²,
L. Schaefer¹²⁴, R. Schaefer⁴⁵, J. Schaeffer⁸⁶, S. Schaepe²³,
S. Schaetzel^{60b}, U. Schäfer⁸⁶, A.C. Schaffer¹¹⁹, D. Schaile¹⁰²,
R.D. Schamberger¹⁵⁰, V. Scharf^{60a}, V.A. Schegelsky¹²⁵, D. Scheirich¹³¹,
M. Schernau¹⁶⁶, C. Schiavi^{53a,53b}, S. Schier¹³⁹, L.K. Schildgen²³,
C. Schillo⁵¹, M. Schioppa^{40a,40b}, S. Schlenker³²,
K.R. Schmidt-Sommerfeld¹⁰³, K. Schmieden³², C. Schmitt⁸⁶,
S. Schmitt⁴⁵, S. Schmitz⁸⁶, U. Schnoor⁵¹, L. Schoeffel¹³⁸,
A. Schoening^{60b}, B.D. Schoenrock⁹³, E. Schopf²³, M. Schott⁸⁶,
J.F.P. Schouwenberg¹⁰⁸, J. Schovancova³², S. Schramm⁵², N. Schuh⁸⁶,
A. Schulte⁸⁶, M.J. Schultens²³, H.-C. Schultz-Coulon^{60a}, H. Schulz¹⁷,
M. Schumacher⁵¹, B.A. Schumm¹³⁹, Ph. Schune¹³⁸, A. Schwartzman¹⁴⁵,
T.A. Schwarz⁹², H. Schweiger⁸⁷, Ph. Schwemling¹³⁸, R. Schwienhorst⁹³,
J. Schwindling¹³⁸, T. Schwindt²³, A. Sciandra²³, G. Sciolla²⁵,
F. Scuri^{126a,126b}, F. Scutti⁹¹, J. Searcy⁹², P. Seema²³, S.C. Seidel¹⁰⁷,
A. Seiden¹³⁹, J.M. Seixas^{26a}, G. Sekhniaidze^{106a}, K. Sekhon⁹²,

S.J. Sekula⁴³, N. Semprini-Cesari^{22a,22b}, S. Senkin³⁷, C. Serfon¹²¹,
 L. Serin¹¹⁹, L. Serkin^{167a,167b}, M. Sessa^{136a,136b}, R. Seuster¹⁷²,
 H. Severini¹¹⁵, T. Sfiligoj⁷⁸, F. Sforza³², A. Sfyrla⁵², E. Shabalina⁵⁷,
 N.W. Shaikh^{148a,148b}, L.Y. Shan^{35a}, R. Shang¹⁶⁹, J.T. Shank²⁴,
 M. Shapiro¹⁶, P.B. Shatalov⁹⁹, K. Shaw^{167a,167b}, S.M. Shaw⁸⁷,
 A. Shcherbakova^{148a,148b}, C.Y. Shehu¹⁵¹, Y. Shen¹¹⁵, P. Sherwood⁸¹,
 L. Shi^{153,ap}, S. Shimizu⁷⁰, C.O. Shimmin¹⁷⁹, M. Shimojima¹⁰⁴,
 I.P.J. Shipsey¹²², S. Shirabe⁷³, M. Shiyakova^{68,aq}, J. Shlomi¹⁷⁵,
 A. Shmeleva⁹⁸, D. Shoaleh Saadi⁹⁷, M.J. Shochet³³, S. Shojaii^{94a},
 D.R. Shope¹¹⁵, S. Shrestha¹¹³, E. Shulga¹⁰⁰, M.A. Shupe⁷, P. Sicho¹²⁹,
 A.M. Sickles¹⁶⁹, P.E. Sidebo¹⁴⁹, E. Sideras Haddad^{147c},
 O. Sidiropoulou¹⁷⁷, D. Sidorov¹¹⁶, A. Sidoti^{22a,22b}, F. Siegert⁴⁷,
 Dj. Sijacki¹⁴, J. Silva^{128a,128d}, S.B. Silverstein^{148a}, V. Simak¹³⁰,
 Lj. Simic¹⁴, S. Simion¹¹⁹, E. Simioni⁸⁶, B. Simmons⁸¹, M. Simon⁸⁶,
 P. Sinervo¹⁶¹, N.B. Sinev¹¹⁸, M. Sioli^{22a,22b}, G. Siragusa¹⁷⁷, I. Siral⁹²,
 S.Yu. Sivoklokov¹⁰¹, J. Sjölin^{148a,148b}, M.B. Skinner⁷⁵, P. Skubic¹¹⁵,
 M. Slater¹⁹, T. Slavicek¹³⁰, M. Slawinska¹⁰⁹, K. Sliwa¹⁶⁵, R. Slovak¹³¹,
 V. Smakhtin¹⁷⁵, B.H. Smart⁵, J. Smiesko^{146a}, N. Smirnov¹⁰⁰,
 S.Yu. Smirnov¹⁰⁰, Y. Smirnov¹⁰⁰, L.N. Smirnova^{101,ar}, O. Smirnova⁸⁴,
 J.W. Smith⁵⁷, M.N.K. Smith³⁸, R.W. Smith³⁸, M. Smizanska⁷⁵,
 K. Smolek¹³⁰, A.A. Snesev⁹⁸, I.M. Snyder¹¹⁸, S. Snyder²⁷,
 R. Sobie^{172,o}, F. Socher⁴⁷, A. Soffer¹⁵⁵, D.A. Soh¹⁵³, G. Sokhrannyi⁷⁸,
 C.A. Solans Sanchez³², M. Solar¹³⁰, E.Yu. Soldatov¹⁰⁰, U. Soldevila¹⁷⁰,
 A.A. Solodkov¹³², A. Soloshenko⁶⁸, O.V. Solovyanov¹³², V. Solovyev¹²⁵,
 P. Sommer⁵¹, H. Son¹⁶⁵, H.Y. Song^{36a,as}, A. Sopczak¹³⁰, D. Sosa^{60b},
 C.L. Sotiropoulou^{126a,126b}, R. Soualah^{167a,167c}, A.M. Soukharev^{111,c},
 D. South⁴⁵, B.C. Sowden⁸⁰, S. Spagnolo^{76a,76b}, M. Spalla^{126a,126b},
 M. Spangenberg¹⁷³, F. Spanò⁸⁰, D. Sperlich¹⁷, F. Spettel¹⁰³,
 T.M. Spieker^{60a}, R. Spighi^{22a}, G. Spigo³², L.A. Spiller⁹¹, M. Spousta¹³¹,
 R.D. St. Denis^{56,*}, A. Stabile^{94a}, R. Stamen^{60a}, S. Stamm¹⁷,
 E. Stanecka⁴², R.W. Stanek⁶, C. Stanescu^{136a}, M.M. Stanitzki⁴⁵,
 S. Stapnes¹²¹, E.A. Starchenko¹³², G.H. Stark³³, J. Stark⁵⁸, S.H. Stark³⁹,
 P. Staroba¹²⁹, P. Starovoitov^{60a}, S. Stärz³², R. Staszewski⁴²,
 P. Steinberg²⁷, B. Stelzer¹⁴⁴, H.J. Stelzer³², O. Stelzer-Chilton^{163a},
 H. Stenzel⁵⁵, G.A. Stewart⁵⁶, M.C. Stockton¹¹⁸, M. Stoebe⁹⁰,
 G. Stoicea^{28b}, P. Stolte⁵⁷, S. Stonjek¹⁰³, A.R. Stradling⁸, A. Straessner⁴⁷,
 M.E. Stramaglia¹⁸, J. Strandberg¹⁴⁹, S. Strandberg^{148a,148b},

A. Strandlie ¹²¹, M. Strauss ¹¹⁵, P. Strizenec ^{146b}, R. Ströhmer ¹⁷⁷,
 D.M. Strom ¹¹⁸, R. Stroynowski ⁴³, A. Strubig ¹⁰⁸, S.A. Stucci ²⁷,
 B. Stugu ¹⁵, N.A. Styles ⁴⁵, D. Su ¹⁴⁵, J. Su ¹²⁷, S. Suchek ^{60a}, Y. Sugaya ¹²⁰,
 M. Suk ¹³⁰, V.V. Sulin ⁹⁸, S. Sultansoy ^{4c}, T. Sumida ⁷¹, S. Sun ⁵⁹, X. Sun ³,
 K. Suruliz ¹⁵¹, C.J.E. Suster ¹⁵², M.R. Sutton ¹⁵¹, S. Suzuki ⁶⁹,
 M. Svatos ¹²⁹, M. Swiatlowski ³³, S.P. Swift ², I. Sykora ^{146a}, T. Sykora ¹³¹,
 D. Ta ⁵¹, K. Tackmann ⁴⁵, J. Taenzer ¹⁵⁵, A. Taffard ¹⁶⁶, R. Tafirout ^{163a},
 N. Taiblum ¹⁵⁵, H. Takai ²⁷, R. Takashima ⁷², T. Takeshita ¹⁴², Y. Takubo ⁶⁹,
 M. Talby ⁸⁸, A.A. Talyshev ^{111,c}, J. Tanaka ¹⁵⁷, M. Tanaka ¹⁵⁹, R. Tanaka ¹¹⁹,
 S. Tanaka ⁶⁹, R. Tanioka ⁷⁰, B.B. Tannenwald ¹¹³, S. Tapia Araya ^{34b},
 S. Tapprogge ⁸⁶, S. Tarem ¹⁵⁴, G.F. Tartarelli ^{94a}, P. Tas ¹³¹, M. Tasevsky ¹²⁹,
 T. Tashiro ⁷¹, E. Tassi ^{40a,40b}, A. Tavares Delgado ^{128a,128b}, Y. Tayalati ^{137e},
 A.C. Taylor ¹⁰⁷, G.N. Taylor ⁹¹, P.T.E. Taylor ⁹¹, W. Taylor ^{163b},
 P. Teixeira-Dias ⁸⁰, D. Temple ¹⁴⁴, H. Ten Kate ³², P.K. Teng ¹⁵³,
 J.J. Teoh ¹²⁰, F. Tepel ¹⁷⁸, S. Terada ⁶⁹, K. Terashi ¹⁵⁷, J. Terron ⁸⁵,
 S. Terzo ¹³, M. Testa ⁵⁰, R.J. Teuscher ^{161,o}, T. Theveneaux-Pelzer ⁸⁸,
 J.P. Thomas ¹⁹, J. Thomas-Wilsker ⁸⁰, P.D. Thompson ¹⁹,
 A.S. Thompson ⁵⁶, L.A. Thomsen ¹⁷⁹, E. Thomson ¹²⁴, M.J. Tibbetts ¹⁶,
 R.E. Ticse Torres ⁸⁸, V.O. Tikhomirov ^{98,at}, Yu.A. Tikhonov ^{111,c},
 S. Timoshenko ¹⁰⁰, P. Tipton ¹⁷⁹, S. Tisserant ⁸⁸, K. Todome ¹⁵⁹,
 S. Todorova-Nova ⁵, J. Tojo ⁷³, S. Tokár ^{146a}, K. Tokushuku ⁶⁹, E. Tolley ⁵⁹,
 L. Tomlinson ⁸⁷, M. Tomoto ¹⁰⁵, L. Tompkins ^{145,au}, K. Toms ¹⁰⁷, B. Tong ⁵⁹,
 P. Tornambe ⁵¹, E. Torrence ¹¹⁸, H. Torres ¹⁴⁴, E. Torró Pastor ¹⁴⁰,
 J. Toth ^{88,av}, F. Touchard ⁸⁸, D.R. Tovey ¹⁴¹, C.J. Treado ¹¹², T. Trefzger ¹⁷⁷,
 F. Tresoldi ¹⁵¹, A. Tricoli ²⁷, I.M. Trigger ^{163a}, S. Trincaz-Duvoid ⁸³,
 M.F. Tripiana ¹³, W. Trischuk ¹⁶¹, B. Trocmé ⁵⁸, A. Trofymov ⁴⁵,
 C. Troncon ^{94a}, M. Trotter-McDonald ¹⁶, M. Trovatelli ¹⁷²,
 L. Truong ^{167a,167c}, M. Trzebinski ⁴², A. Trzupek ⁴², K.W. Tsang ^{62a},
 J.C-L. Tseng ¹²², P.V. Tsiarehshka ⁹⁵, G. Tsipolitis ¹⁰, N. Tsirintanis ⁹,
 S. Tsiskaridze ¹³, V. Tsiskaridze ⁵¹, E.G. Tskhadadze ^{54a}, K.M. Tsui ^{62a},
 I.I. Tsukerman ⁹⁹, V. Tsulaia ¹⁶, S. Tsuno ⁶⁹, D. Tsybychev ¹⁵⁰, Y. Tu ^{62b},
 A. Tudorache ^{28b}, V. Tudorache ^{28b}, T.T. Tulbure ^{28a}, A.N. Tuna ⁵⁹,
 S.A. Tuppiti ^{22a,22b}, S. Turchikhin ⁶⁸, D. Turgeman ¹⁷⁵, I. Turk Cakir ^{4b,aw},
 R. Turra ^{94a}, P.M. Tuts ³⁸, G. Uchielli ^{22a,22b}, I. Ueda ⁶⁹,
 M. Ughetto ^{148a,148b}, F. Ukegawa ¹⁶⁴, G. Unal ³², A. Undrus ²⁷, G. Unel ¹⁶⁶,
 F.C. Ungaro ⁹¹, Y. Unno ⁶⁹, C. Unverdorben ¹⁰², J. Urban ^{146b}, P. Urquijo ⁹¹,
 P. Urrejola ⁸⁶, G. Usai ⁸, J. Usui ⁶⁹, L. Vacavant ⁸⁸, V. Vacek ¹³⁰,

B. Vachon⁹⁰, C. Valderanis¹⁰², E. Valdes Santurio^{148a,148b},
 S. Valentinetti^{22a,22b}, A. Valero¹⁷⁰, L. Valéry¹³, S. Valkar¹³¹, A. Vallier⁵,
 J.A. Valls Ferrer¹⁷⁰, W. Van Den Wollenberg¹⁰⁹, H. van der Graaf¹⁰⁹,
 N. van Eldik¹⁵⁴, P. van Gemmeren⁶, J. Van Nieuwkoop¹⁴⁴,
 I. van Vulpen¹⁰⁹, M.C. van Woerden¹⁰⁹, M. Vanadia^{135a,135b},
 W. Vandelli³², R. Vanguri¹²⁴, A. Vaniachine¹⁶⁰, P. Vankov¹⁰⁹,
 G. Vardanyan¹⁸⁰, R. Vari^{134a}, E.W. Varnes⁷, C. Varni^{53a,53b}, T. Varol⁴³,
 D. Varouchas¹¹⁹, A. Vartapetian⁸, K.E. Varvell¹⁵², J.G. Vasquez¹⁷⁹,
 G.A. Vasquez^{34b}, F. Vazeille³⁷, T. Vazquez Schroeder⁹⁰, J. Veatch⁵⁷,
 V. Veeraraghavan⁷, L.M. Veloce¹⁶¹, F. Veloso^{128a,128c}, S. Veneziano^{134a},
 A. Ventura^{76a,76b}, M. Venturi¹⁷², N. Venturi¹⁶¹, A. Venturini²⁵,
 V. Vercesi^{123a}, M. Verducci^{136a,136b}, W. Verkerke¹⁰⁹, J.C. Vermeulen¹⁰⁹,
 M.C. Vetterli^{144,d}, N. Viaux Maira^{34b}, O. Viazlo⁸⁴, I. Vichou^{169,*},
 T. Vickey¹⁴¹, O.E. Vickey Boeriu¹⁴¹, G.H.A. Viehhauser¹²², S. Viel¹⁶,
 L. Vigani¹²², M. Villa^{22a,22b}, M. Villaplana Perez^{94a,94b}, E. Vilucchi⁵⁰,
 M.G. Vincter³¹, V.B. Vinogradov⁶⁸, A. Vishwakarma⁴⁵, C. Vittori^{22a,22b},
 I. Vivarelli¹⁵¹, S. Vlachos¹⁰, M. Vlasak¹³⁰, M. Vogel¹⁷⁸, P. Vokac¹³⁰,
 G. Volpi^{126a,126b}, H. von der Schmitt¹⁰³, E. von Toerne²³, V. Vorobel¹³¹,
 K. Vorobev¹⁰⁰, M. Vos¹⁷⁰, R. Voss³², J.H. Vossebeld⁷⁷, N. Vranjes¹⁴,
 M. Vranjes Milosavljevic¹⁴, V. Vrba¹³⁰, M. Vreeswijk¹⁰⁹,
 R. Vuillermet³², I. Vukotic³³, P. Wagner²³, W. Wagner¹⁷⁸,
 J. Wagner-Kuhr¹⁰², H. Wahlberg⁷⁴, S. Wahrmund⁴⁷, J. Wakabayashi¹⁰⁵,
 J. Walder⁷⁵, R. Walker¹⁰², W. Walkowiak¹⁴³, V. Wallangen^{148a,148b},
 C. Wang^{35b}, C. Wang^{36b,ax}, F. Wang¹⁷⁶, H. Wang¹⁶, H. Wang³,
 J. Wang⁴⁵, J. Wang¹⁵², Q. Wang¹¹⁵, R. Wang⁶, S.M. Wang¹⁵³, T. Wang³⁸,
 W. Wang^{153,ay}, W. Wang^{36a}, Z. Wang^{36c}, C. Wanotayaroj¹¹⁸,
 A. Warburton⁹⁰, C.P. Ward³⁰, D.R. Wardrope⁸¹, A. Washbrook⁴⁹,
 P.M. Watkins¹⁹, A.T. Watson¹⁹, M.F. Watson¹⁹, G. Watts¹⁴⁰, S. Watts⁸⁷,
 B.M. Waugh⁸¹, A.F. Webb¹¹, S. Webb⁸⁶, M.S. Weber¹⁸, S.W. Weber¹⁷⁷,
 S.A. Weber³¹, J.S. Webster⁶, A.R. Weidberg¹²², B. Weinert⁶⁴,
 J. Weingarten⁵⁷, C. Weiser⁵¹, H. Weits¹⁰⁹, P.S. Wells³², T. Wenaus²⁷,
 T. Wengler³², S. Wenig³², N. Vermes²³, M.D. Werner⁶⁷, P. Werner³²,
 M. Wessels^{60a}, K. Whalen¹¹⁸, N.L. Whallon¹⁴⁰, A.M. Wharton⁷⁵,
 A. White⁸, M.J. White¹, R. White^{34b}, D. Whiteson¹⁶⁶, F.J. Wickens¹³³,
 W. Wiedenmann¹⁷⁶, M. Wielers¹³³, C. Wiglesworth³⁹,
 L.A.M. Wiik-Fuchs²³, A. Wildauer¹⁰³, F. Wilk⁸⁷, H.G. Wilkens³²,
 H.H. Williams¹²⁴, S. Williams¹⁰⁹, C. Willis⁹³, S. Willocq⁸⁹,

J.A. Wilson¹⁹, I. Wingerter-Seez⁵, E. Winkels¹⁵¹, F. Winklmeier¹¹⁸,
 O.J. Winston¹⁵¹, B.T. Winter²³, M. Wittgen¹⁴⁵, M. Wobisch^{82,v},
 T.M.H. Wolf¹⁰⁹, R. Wolff⁸⁸, M.W. Wolter⁴², H. Wolters^{128a,128c},
 V.W.S. Wong¹⁷¹, S.D. Worm¹⁹, B.K. Wosiek⁴², J. Wotschack³²,
 K.W. Wozniak⁴², M. Wu³³, S.L. Wu¹⁷⁶, X. Wu⁵², Y. Wu⁹², T.R. Wyatt⁸⁷,
 B.M. Wynne⁴⁹, S. Xella³⁹, Z. Xi⁹², L. Xia^{35c}, D. Xu^{35a}, L. Xu²⁷,
 B. Yabsley¹⁵², S. Yacoob^{147a}, D. Yamaguchi¹⁵⁹, Y. Yamaguchi¹²⁰,
 A. Yamamoto⁶⁹, S. Yamamoto¹⁵⁷, T. Yamanaka¹⁵⁷, K. Yamauchi¹⁰⁵,
 Y. Yamazaki⁷⁰, Z. Yan²⁴, H. Yang^{36c}, H. Yang¹⁶, Y. Yang¹⁵³, Z. Yang¹⁵,
 W-M. Yao¹⁶, Y.C. Yap⁸³, Y. Yasu⁶⁹, E. Yatsenko⁵, K.H. Yau Wong²³,
 J. Ye⁴³, S. Ye²⁷, I. Yeletsikh⁶⁸, E. Yigitbasi²⁴, E. Yildirim⁸⁶,
 K. Yorita¹⁷⁴, K. Yoshihara¹²⁴, C. Young¹⁴⁵, C.J.S. Young³², D.R. Yu¹⁶,
 J. Yu⁸, J. Yu⁶⁷, S.P.Y. Yuen²³, I. Yusuf^{30,az}, B. Zabinski⁴²,
 G. Zacharis¹⁰, R. Zaidan¹³, A.M. Zaitsev^{132,am}, N. Zakharchuk⁴⁵,
 J. Zalieckas¹⁵, A. Zaman¹⁵⁰, S. Zambito⁵⁹, D. Zanzi⁹¹, C. Zeitnitz¹⁷⁸,
 M. Zeman¹³⁰, A. Zemla^{41a}, J.C. Zeng¹⁶⁹, Q. Zeng¹⁴⁵, O. Zenin¹³²,
 T. Ženiš^{146a}, D. Zerwas¹¹⁹, D. Zhang⁹², F. Zhang¹⁷⁶, G. Zhang^{36a,as},
 H. Zhang^{35b}, J. Zhang⁶, L. Zhang⁵¹, L. Zhang^{36a}, M. Zhang¹⁶⁹,
 R. Zhang²³, R. Zhang^{36a,ax}, X. Zhang^{36b}, Y. Zhang^{35a}, Z. Zhang¹¹⁹,
 X. Zhao⁴³, Y. Zhao^{36b,ba}, Z. Zhao^{36a}, A. Zhemchugov⁶⁸, J. Zhong¹²²,
 B. Zhou⁹², C. Zhou¹⁷⁶, L. Zhou⁴³, M. Zhou^{35a}, M. Zhou¹⁵⁰, N. Zhou^{35c},
 C.G. Zhu^{36b}, H. Zhu^{35a}, J. Zhu⁹², Y. Zhu^{36a}, X. Zhuang^{35a}, K. Zhukov⁹⁸,
 A. Zibell¹⁷⁷, D. Zieminska⁶⁴, N.I. Zimine⁶⁸, C. Zimmermann⁸⁶,
 S. Zimmermann⁵¹, Z. Zinonos¹⁰³, M. Zinser⁸⁶, M. Ziolkowski¹⁴³,
 L. Živković¹⁴, G. Zobernig¹⁷⁶, A. Zoccoli^{22a,22b}, R. Zou³³,
 M. zur Nedden¹⁷, L. Zwalinski³²

¹ Department of Physics, University of Adelaide, Adelaide, Australia

² Physics Department, SUNY Albany, Albany, NY, United States of America

³ Department of Physics, University of Alberta, Edmonton, AB, Canada

⁴ (a) Department of Physics, Ankara University, Ankara; (b) Istanbul Aydin University, Istanbul; (c) Division of Physics, TOBB University of Economics and Technology, Ankara, Turkey

⁵ LAPP, CNRS/IN2P3 and Université Savoie Mont Blanc, Annecy-le-Vieux, France

⁶ High Energy Physics Division, Argonne National Laboratory, Argonne, IL, United States of America

⁷ Department of Physics, University of Arizona, Tucson, AZ, United States of America

⁸ Department of Physics, The University of Texas at Arlington, Arlington, TX, United States of America

⁹ Physics Department, National and Kapodistrian University of Athens, Athens, Greece

¹⁰ Physics Department, National Technical University of Athens, Zografou, Greece

¹¹ Department of Physics, The University of Texas at Austin, Austin, TX, United States of America

¹² Institute of Physics, Azerbaijan Academy of Sciences, Baku, Azerbaijan

¹³ Institut de Física d'Altes Energies (IFAE), The Barcelona Institute of Science and Technology, Barcelona, Spain

¹⁴ Institute of Physics, University of Belgrade, Belgrade, Serbia

¹⁵ Department for Physics and Technology, University of Bergen, Bergen, Norway

- ¹⁶ *Physics Division, Lawrence Berkeley National Laboratory and University of California, Berkeley, CA, United States of America*
- ¹⁷ *Department of Physics, Humboldt University, Berlin, Germany*
- ¹⁸ *Albert Einstein Center for Fundamental Physics and Laboratory for High Energy Physics, University of Bern, Bern, Switzerland*
- ¹⁹ *School of Physics and Astronomy, University of Birmingham, Birmingham, United Kingdom*
- ²⁰ ^(a) *Department of Physics, Bogazici University, Istanbul;* ^(b) *Department of Physics Engineering, Gaziantep University, Gaziantep;* ^(d) *Istanbul Bilgi University, Faculty of Engineering and Natural Sciences, Istanbul;* ^(e) *Bahcesehir University, Faculty of Engineering and Natural Sciences, Istanbul, Turkey*
- ²¹ *Centro de Investigaciones, Universidad Antonio Narino, Bogota, Colombia*
- ²² ^(a) *INFN Sezione di Bologna;* ^(b) *Dipartimento di Fisica e Astronomia, Università di Bologna, Bologna, Italy*
- ²³ *Physikalisches Institut, University of Bonn, Bonn, Germany*
- ²⁴ *Department of Physics, Boston University, Boston, MA, United States of America*
- ²⁵ *Department of Physics, Brandeis University, Waltham, MA, United States of America*
- ²⁶ ^(a) *Universidade Federal do Rio De Janeiro COPPE/EE/IF, Rio de Janeiro;* ^(b) *Electrical Circuits Department, Federal University of Juiz de Fora (UFJF), Juiz de Fora;* ^(c) *Federal University of Sao Joao del Rei (UFSJ), Sao Joao del Rei;* ^(d) *Instituto de Fisica, Universidade de Sao Paulo, Sao Paulo, Brazil*
- ²⁷ *Physics Department, Brookhaven National Laboratory, Upton, NY, United States of America*
- ²⁸ ^(a) *Transilvania University of Brasov, Brasov;* ^(b) *Horia Hulubei National Institute of Physics and Nuclear Engineering, Bucharest;* ^(c) *Department of Physics, Alexandru Ioan Cuza University of Iasi, Iasi;* ^(d) *National Institute for Research and Development of Isotopic and Molecular Technologies, Physics Department, Cluj Napoca;* ^(e) *University Politehnica Bucharest, Bucharest;* ^(f) *West University in Timisoara, Timisoara, Romania*
- ²⁹ *Departamento de Física, Universidad de Buenos Aires, Buenos Aires, Argentina*
- ³⁰ *Cavendish Laboratory, University of Cambridge, Cambridge, United Kingdom*
- ³¹ *Department of Physics, Carleton University, Ottawa, ON, Canada*
- ³² *CERN, Geneva, Switzerland*
- ³³ *Enrico Fermi Institute, University of Chicago, Chicago, IL, United States of America*
- ³⁴ ^(a) *Departamento de Física, Pontificia Universidad Católica de Chile, Santiago;* ^(b) *Departamento de Física, Universidad Técnica Federico Santa María, Valparaíso, Chile*
- ³⁵ ^(a) *Institute of High Energy Physics, Chinese Academy of Sciences, Beijing;* ^(b) *Department of Physics, Nanjing University, Jiangsu;* ^(c) *Physics Department, Tsinghua University, Beijing 100084, China*
- ³⁶ ^(a) *Department of Modern Physics and State Key Laboratory of Particle Detection and Electronics, University of Science and Technology of China, Anhui;* ^(b) *School of Physics, Shandong University, Shandong;* ^(c) *Department of Physics and Astronomy, Key Laboratory for Particle Physics, Astrophysics and Cosmology, Ministry of Education; Shanghai Key Laboratory for Particle Physics and Cosmology, Shanghai Jiao Tong University, Shanghai (also at PKU-CHEP), China*
- ³⁷ *Université Clermont Auvergne, CNRS/IN2P3, LPC, Clermont-Ferrand, France*
- ³⁸ *Nevis Laboratory, Columbia University, Irvington, NY, United States of America*
- ³⁹ *Niels Bohr Institute, University of Copenhagen, Kobenhavn, Denmark*
- ⁴⁰ ^(a) *INFN Gruppo Collegato di Cosenza, Laboratori Nazionali di Frascati;* ^(b) *Dipartimento di Fisica, Università della Calabria, Rende, Italy*
- ⁴¹ ^(a) *AGH University of Science and Technology, Faculty of Physics and Applied Computer Science, Krakow;* ^(b) *Marian Smoluchowski Institute of Physics, Jagiellonian University, Krakow, Poland*
- ⁴² *Institute of Nuclear Physics Polish Academy of Sciences, Krakow, Poland*
- ⁴³ *Physics Department, Southern Methodist University, Dallas, TX, United States of America*
- ⁴⁴ *Physics Department, University of Texas at Dallas, Richardson, TX, United States of America*
- ⁴⁵ *DESY, Hamburg and Zeuthen, Germany*
- ⁴⁶ *Lehrstuhl für Experimentelle Physik IV, Technische Universität Dortmund, Dortmund, Germany*
- ⁴⁷ *Institut für Kern- und Teilchenphysik, Technische Universität Dresden, Dresden, Germany*
- ⁴⁸ *Department of Physics, Duke University, Durham, NC, United States of America*
- ⁴⁹ *SUPA – School of Physics and Astronomy, University of Edinburgh, Edinburgh, United Kingdom*
- ⁵⁰ *INFN e Laboratori Nazionali di Frascati, Frascati, Italy*
- ⁵¹ *Fakultät für Mathematik und Physik, Albert-Ludwigs-Universität, Freiburg, Germany*
- ⁵² *Departement de Physique Nucleaire et Corpusculaire, Université de Genève, Geneva, Switzerland*
- ⁵³ ^(a) *INFN Sezione di Genova;* ^(b) *Dipartimento di Fisica, Università di Genova, Genova, Italy*

- 54 ^(a) E. Andronikashvili Institute of Physics, Iv. Javakhishvili Tbilisi State University, Tbilisi; ^(b) High Energy Physics Institute, Tbilisi State University, Tbilisi, Georgia
- 55 II Physikalisches Institut, Justus-Liebig-Universität Giessen, Giessen, Germany
- 56 SUPA – School of Physics and Astronomy, University of Glasgow, Glasgow, United Kingdom
- 57 II Physikalisches Institut, Georg-August-Universität, Göttingen, Germany
- 58 Laboratoire de Physique Subatomique et de Cosmologie, Université Grenoble-Alpes, CNRS/IN2P3, Grenoble, France
- 59 Laboratory for Particle Physics and Cosmology, Harvard University, Cambridge, MA, United States of America
- 60 ^(a) Kirchhoff-Institut für Physik, Ruprecht-Karls-Universität Heidelberg, Heidelberg; ^(b) Physikalisches Institut, Ruprecht-Karls-Universität Heidelberg, Heidelberg; ^(c) ZITI Institut für technische Informatik, Ruprecht-Karls-Universität Heidelberg, Mannheim, Germany
- 61 Faculty of Applied Information Science, Hiroshima Institute of Technology, Hiroshima, Japan
- 62 ^(a) Department of Physics, The Chinese University of Hong Kong, Shatin, N.T., Hong Kong; ^(b) Department of Physics, The University of Hong Kong, Hong Kong; ^(c) Department of Physics and Institute for Advanced Study, The Hong Kong University of Science and Technology, Clear Water Bay, Kowloon, Hong Kong, China
- 63 Department of Physics, National Tsing Hua University, Taiwan, Taiwan
- 64 Department of Physics, Indiana University, Bloomington, IN, United States of America
- 65 Institut für Astro- und Teilchenphysik, Leopold-Franzens-Universität, Innsbruck, Austria
- 66 University of Iowa, Iowa City, IA, United States of America
- 67 Department of Physics and Astronomy, Iowa State University, Ames, IA, United States of America
- 68 Joint Institute for Nuclear Research, JINR Dubna, Dubna, Russia
- 69 KEK, High Energy Accelerator Research Organization, Tsukuba, Japan
- 70 Graduate School of Science, Kobe University, Kobe, Japan
- 71 Faculty of Science, Kyoto University, Kyoto, Japan
- 72 Kyoto University of Education, Kyoto, Japan
- 73 Research Center for Advanced Particle Physics and Department of Physics, Kyushu University, Fukuoka, Japan
- 74 Instituto de Física La Plata, Universidad Nacional de La Plata and CONICET, La Plata, Argentina
- 75 Physics Department, Lancaster University, Lancaster, United Kingdom
- 76 ^(a) INFN Sezione di Lecce; ^(b) Dipartimento di Matematica e Fisica, Università del Salento, Lecce, Italy
- 77 Oliver Lodge Laboratory, University of Liverpool, Liverpool, United Kingdom
- 78 Department of Experimental Particle Physics, Jožef Stefan Institute and Department of Physics, University of Ljubljana, Ljubljana, Slovenia
- 79 School of Physics and Astronomy, Queen Mary University of London, London, United Kingdom
- 80 Department of Physics, Royal Holloway University of London, Surrey, United Kingdom
- 81 Department of Physics and Astronomy, University College London, London, United Kingdom
- 82 Louisiana Tech University, Ruston, LA, United States of America
- 83 Laboratoire de Physique Nucléaire et de Hautes Energies, UPMC and Université Paris-Diderot and CNRS/IN2P3, Paris, France
- 84 Fysiska institutionen, Lunds universitet, Lund, Sweden
- 85 Departamento de Física Teórica C-15, Universidad Autónoma de Madrid, Madrid, Spain
- 86 Institut für Physik, Universität Mainz, Mainz, Germany
- 87 School of Physics and Astronomy, University of Manchester, Manchester, United Kingdom
- 88 CPPM, Aix-Marseille Université and CNRS/IN2P3, Marseille, France
- 89 Department of Physics, University of Massachusetts, Amherst, MA, United States of America
- 90 Department of Physics, McGill University, Montreal, QC, Canada
- 91 School of Physics, University of Melbourne, Victoria, Australia
- 92 Department of Physics, The University of Michigan, Ann Arbor, MI, United States of America
- 93 Department of Physics and Astronomy, Michigan State University, East Lansing, MI, United States of America
- 94 ^(a) INFN Sezione di Milano; ^(b) Dipartimento di Fisica, Università di Milano, Milano, Italy
- 95 B.I. Stepanov Institute of Physics, National Academy of Sciences of Belarus, Minsk, Belarus
- 96 Research Institute for Nuclear Problems of Byelorussian State University, Minsk, Belarus
- 97 Group of Particle Physics, University of Montreal, Montreal, QC, Canada
- 98 P.N. Lebedev Physical Institute of the Russian Academy of Sciences, Moscow, Russia
- 99 Institute for Theoretical and Experimental Physics (ITEP), Moscow, Russia
- 100 National Research Nuclear University MEPhI, Moscow, Russia
- 101 D.V. Skobeltsyn Institute of Nuclear Physics, M.V. Lomonosov Moscow State University, Moscow, Russia

- 102 Fakultät für Physik, Ludwig-Maximilians-Universität München, München, Germany
- 103 Max-Planck-Institut für Physik (Werner-Heisenberg-Institut), München, Germany
- 104 Nagasaki Institute of Applied Science, Nagasaki, Japan
- 105 Graduate School of Science and Kobayashi–Maskawa Institute, Nagoya University, Nagoya, Japan
- 106 (a) INFN Sezione di Napoli; (b) Dipartimento di Fisica, Università di Napoli, Napoli, Italy
- 107 Department of Physics and Astronomy, University of New Mexico, Albuquerque, NM, United States of America
- 108 Institute for Mathematics, Astrophysics and Particle Physics, Radboud University Nijmegen/Nikhef, Nijmegen, Netherlands
- 109 Nikhef National Institute for Subatomic Physics and University of Amsterdam, Amsterdam, Netherlands
- 110 Department of Physics, Northern Illinois University, DeKalb, IL, United States of America
- 111 Budker Institute of Nuclear Physics, SB RAS, Novosibirsk, Russia
- 112 Department of Physics, New York University, New York, NY, United States of America
- 113 Ohio State University, Columbus, OH, United States of America
- 114 Faculty of Science, Okayama University, Okayama, Japan
- 115 Homer L. Dodge Department of Physics and Astronomy, University of Oklahoma, Norman, OK, United States of America
- 116 Department of Physics, Oklahoma State University, Stillwater, OK, United States of America
- 117 Palacký University, RCPTM, Olomouc, Czech Republic
- 118 Center for High Energy Physics, University of Oregon, Eugene, OR, United States of America
- 119 LAL, Univ. Paris-Sud, CNRS/IN2P3, Université Paris-Saclay, Orsay, France
- 120 Graduate School of Science, Osaka University, Osaka, Japan
- 121 Department of Physics, University of Oslo, Oslo, Norway
- 122 Department of Physics, Oxford University, Oxford, United Kingdom
- 123 (a) INFN Sezione di Pavia; (b) Dipartimento di Fisica, Università di Pavia, Pavia, Italy
- 124 Department of Physics, University of Pennsylvania, Philadelphia, PA, United States of America
- 125 National Research Centre “Kurchatov Institute” B.P. Konstantinov Petersburg Nuclear Physics Institute, St. Petersburg, Russia
- 126 (a) INFN Sezione di Pisa; (b) Dipartimento di Fisica E. Fermi, Università di Pisa, Pisa, Italy
- 127 Department of Physics and Astronomy, University of Pittsburgh, Pittsburgh, PA, United States of America
- 128 (a) Laboratório de Instrumentação e Física Experimental de Partículas – LIP, Lisboa; (b) Faculdade de Ciências, Universidade de Lisboa, Lisboa; (c) Department of Physics, University of Coimbra, Coimbra; (d) Centro de Física Nuclear da Universidade de Lisboa, Lisboa; (e) Departamento de Física, Universidade do Minho, Braga; (f) Departamento de Física Teórica y del Cosmos and CAFPE, Universidad de Granada, Granada; (g) Dep. Física and CEFITEC of Faculdade de Ciências e Tecnologia, Universidade Nova de Lisboa, Caparica, Portugal
- 129 Institute of Physics, Academy of Sciences of the Czech Republic, Praha, Czech Republic
- 130 Czech Technical University in Prague, Praha, Czech Republic
- 131 Charles University, Faculty of Mathematics and Physics, Prague, Czech Republic
- 132 State Research Center Institute for High Energy Physics (Protvino), NRC KI, Russia
- 133 Particle Physics Department, Rutherford Appleton Laboratory, Didcot, United Kingdom
- 134 (a) INFN Sezione di Roma; (b) Dipartimento di Fisica, Sapienza Università di Roma, Roma, Italy
- 135 (a) INFN Sezione di Roma Tor Vergata; (b) Dipartimento di Fisica, Università di Roma Tor Vergata, Roma, Italy
- 136 (a) INFN Sezione di Roma Tre; (b) Dipartimento di Matematica e Fisica, Università Roma Tre, Roma, Italy
- 137 (a) Faculté des Sciences Ain Chock, Réseau Universitaire de Physique des Hautes Energies – Université Hassan II, Casablanca; (b) Centre National de l’Energie des Sciences Techniques Nucleaires, Rabat; (c) Faculté des Sciences Semlalia, Université Cadi Ayyad, LPHEA, Marrakech; (d) Faculté des Sciences, Université Mohamed Premier and LPTPM, Oujda; (e) Faculté des sciences, Université Mohammed V, Rabat, Morocco
- 138 DSM/IRFU (Institut de Recherches sur les Lois Fondamentales de l’Univers), CEA Saclay (Commissariat à l’Energie Atomique et aux Energies Alternatives), Gif-sur-Yvette, France
- 139 Santa Cruz Institute for Particle Physics, University of California Santa Cruz, Santa Cruz, CA, United States of America
- 140 Department of Physics, University of Washington, Seattle, WA, United States of America
- 141 Department of Physics and Astronomy, University of Sheffield, Sheffield, United Kingdom
- 142 Department of Physics, Shinshu University, Nagano, Japan
- 143 Department Physik, Universität Siegen, Siegen, Germany
- 144 Department of Physics, Simon Fraser University, Burnaby, BC, Canada
- 145 SLAC National Accelerator Laboratory, Stanford, CA, United States of America

- 146 (a) Faculty of Mathematics, Physics & Informatics, Comenius University, Bratislava; (b) Department of Subnuclear Physics, Institute of Experimental Physics of the Slovak Academy of Sciences, Kosice, Slovak Republic
- 147 (a) Department of Physics, University of Cape Town, Cape Town; (b) Department of Physics, University of Johannesburg, Johannesburg; (c) School of Physics, University of the Witwatersrand, Johannesburg, South Africa
- 148 (a) Department of Physics, Stockholm University; (b) The Oskar Klein Centre, Stockholm, Sweden
- 149 Physics Department, Royal Institute of Technology, Stockholm, Sweden
- 150 Departments of Physics & Astronomy and Chemistry, Stony Brook University, Stony Brook, NY, United States of America
- 151 Department of Physics and Astronomy, University of Sussex, Brighton, United Kingdom
- 152 School of Physics, University of Sydney, Sydney, Australia
- 153 Institute of Physics, Academia Sinica, Taipei, Taiwan
- 154 Department of Physics, Technion: Israel Institute of Technology, Haifa, Israel
- 155 Raymond and Beverly Sackler School of Physics and Astronomy, Tel Aviv University, Tel Aviv, Israel
- 156 Department of Physics, Aristotle University of Thessaloniki, Thessaloniki, Greece
- 157 International Center for Elementary Particle Physics and Department of Physics, The University of Tokyo, Tokyo, Japan
- 158 Graduate School of Science and Technology, Tokyo Metropolitan University, Tokyo, Japan
- 159 Department of Physics, Tokyo Institute of Technology, Tokyo, Japan
- 160 Tomsk State University, Tomsk, Russia
- 161 Department of Physics, University of Toronto, Toronto, ON, Canada
- 162 (a) INFN-TIFPA; (b) University of Trento, Trento, Italy
- 163 (a) TRIUMF, Vancouver, BC; (b) Department of Physics and Astronomy, York University, Toronto, ON, Canada
- 164 Faculty of Pure and Applied Sciences, and Center for Integrated Research in Fundamental Science and Engineering, University of Tsukuba, Tsukuba, Japan
- 165 Department of Physics and Astronomy, Tufts University, Medford, MA, United States of America
- 166 Department of Physics and Astronomy, University of California Irvine, Irvine, CA, United States of America
- 167 (a) INFN Gruppo Collegato di Udine, Sezione di Trieste, Udine; (b) ICTP, Trieste; (c) Dipartimento di Chimica, Fisica e Ambiente, Università di Udine, Udine, Italy
- 168 Department of Physics and Astronomy, University of Uppsala, Uppsala, Sweden
- 169 Department of Physics, University of Illinois, Urbana, IL, United States of America
- 170 Instituto de Física Corpuscular (IFIC), Centro Mixto Universidad de Valencia – CSIC, Spain
- 171 Department of Physics, University of British Columbia, Vancouver, BC, Canada
- 172 Department of Physics and Astronomy, University of Victoria, Victoria, BC, Canada
- 173 Department of Physics, University of Warwick, Coventry, United Kingdom
- 174 Waseda University, Tokyo, Japan
- 175 Department of Particle Physics, The Weizmann Institute of Science, Rehovot, Israel
- 176 Department of Physics, University of Wisconsin, Madison, WI, United States of America
- 177 Fakultät für Physik und Astronomie, Julius-Maximilians-Universität, Würzburg, Germany
- 178 Fakultät für Mathematik und Naturwissenschaften, Fachgruppe Physik, Bergische Universität Wuppertal, Wuppertal, Germany
- 179 Department of Physics, Yale University, New Haven, CT, United States of America
- 180 Yerevan Physics Institute, Yerevan, Armenia
- 181 Centre de Calcul de l'Institut National de Physique Nucléaire et de Physique des Particules (IN2P3), Villeurbanne, France

^a Also at Department of Physics, King's College London, London, United Kingdom.

^b Also at Institute of Physics, Azerbaijan Academy of Sciences, Baku, Azerbaijan.

^c Also at Novosibirsk State University, Novosibirsk, Russia.

^d Also at TRIUMF, Vancouver, BC, Canada.

^e Also at Department of Physics & Astronomy, University of Louisville, Louisville, KY, United States of America.

^f Also at Physics Department, An-Najah National University, Nablus, Palestine.

^g Also at Department of Physics, California State University, Fresno, CA, United States of America.

^h Also at Department of Physics, University of Fribourg, Fribourg, Switzerland.

ⁱ Also at II Physikalisches Institut, Georg-August-Universität, Göttingen, Germany.

- j* Also at Departament de Física de la Universitat Autònoma de Barcelona, Barcelona, Spain.
- k* Also at Departamento de Física e Astronomia, Faculdade de Ciências, Universidade do Porto, Portugal.
- l* Also at Tomsk State University, Tomsk, Russia.
- m* Also at The Collaborative Innovation Center of Quantum Matter (CICQM), Beijing, China.
- n* Also at Università di Napoli Parthenope, Napoli, Italy.
- o* Also at Institute of Particle Physics (IPP), Canada.
- p* Also at Horia Hulubei National Institute of Physics and Nuclear Engineering, Bucharest, Romania.
- q* Also at Department of Physics, St. Petersburg State Polytechnical University, St. Petersburg, Russia.
- r* Also at Borough of Manhattan Community College, City University of New York, New York City, United States of America.
- s* Also at Department of Physics, The University of Michigan, Ann Arbor, MI, United States of America.
- t* Also at Department of Financial and Management Engineering, University of the Aegean, Chios, Greece.
- u* Also at Centre for High Performance Computing, CSIR Campus, Rosebank, Cape Town, South Africa.
- v* Also at Louisiana Tech University, Ruston, LA, United States of America.
- w* Also at Institutio Catalana de Recerca i Estudis Avancats, ICREA, Barcelona, Spain.
- x* Also at Graduate School of Science, Osaka University, Osaka, Japan.
- y* Also at Fakultät für Mathematik und Physik, Albert-Ludwigs-Universität, Freiburg, Germany.
- z* Also at Institute for Mathematics, Astrophysics and Particle Physics, Radboud University Nijmegen/Nikhef, Nijmegen, Netherlands.
- aa* Also at Department of Physics, The University of Texas at Austin, Austin, TX, United States of America.
- ab* Also at Institute of Theoretical Physics, Ilia State University, Tbilisi, Georgia.
- ac* Also at CERN, Geneva, Switzerland.
- ad* Also at Georgian Technical University (GTU), Tbilisi, Georgia.
- ae* Also at Ochadai Academic Production, Ochanomizu University, Tokyo, Japan.
- af* Also at Manhattan College, New York, NY, United States of America.
- ag* Also at Departamento de Física, Pontificia Universidad Católica de Chile, Santiago, Chile.
- ah* Also at Academia Sinica Grid Computing, Institute of Physics, Academia Sinica, Taipei, Taiwan.
- ai* Also at The City College of New York, New York, NY, United States of America.
- aj* Also at School of Physics, Shandong University, Shandong, China.
- ak* Also at Departamento de Física Teórica y del Cosmos and CAFPE, Universidad de Granada, Granada, Spain.
- al* Also at Department of Physics, California State University, Sacramento, CA, United States of America.
- am* Also at Moscow Institute of Physics and Technology State University, Dolgoprudny, Russia.
- an* Also at Departement de Physique Nucleaire et Corpusculaire, Université de Genève, Geneva, Switzerland.
- ao* Also at Institut de Física d'Altes Energies (IFAE), The Barcelona Institute of Science and Technology, Barcelona, Spain.
- ap* Also at School of Physics, Sun Yat-sen University, Guangzhou, China.
- aq* Also at Institute for Nuclear Research and Nuclear Energy (INRNE) of the Bulgarian Academy of Sciences, Sofia, Bulgaria.
- ar* Also at Faculty of Physics, M.V. Lomonosov Moscow State University, Moscow, Russia.
- as* Also at Institute of Physics, Academia Sinica, Taipei, Taiwan.
- at* Also at National Research Nuclear University MEPhI, Moscow, Russia.
- au* Also at Department of Physics, Stanford University, Stanford, CA, United States of America.
- av* Also at Institute for Particle and Nuclear Physics, Wigner Research Centre for Physics, Budapest, Hungary.
- aw* Also at Giresun University, Faculty of Engineering, Turkey.
- ax* Also at CPPM, Aix-Marseille Université and CNRS/IN2P3, Marseille, France.
- ay* Also at Department of Physics, Nanjing University, Jiangsu, China.
- az* Also at University of Malaya, Department of Physics, Kuala Lumpur, Malaysia.
- ba* Also at LAL, Univ. Paris-Sud, CNRS/IN2P3, Université Paris-Saclay, Orsay, France.
- * Deceased.